Deuteron photodisintegration @HIγS below 20 MeV

Henry R. Weller

Duke University and Triangle Universities Nuclear Laboratory

HIγS PROGRAM

HUGS_2, June 2009

The Upgraded HIγS Facility

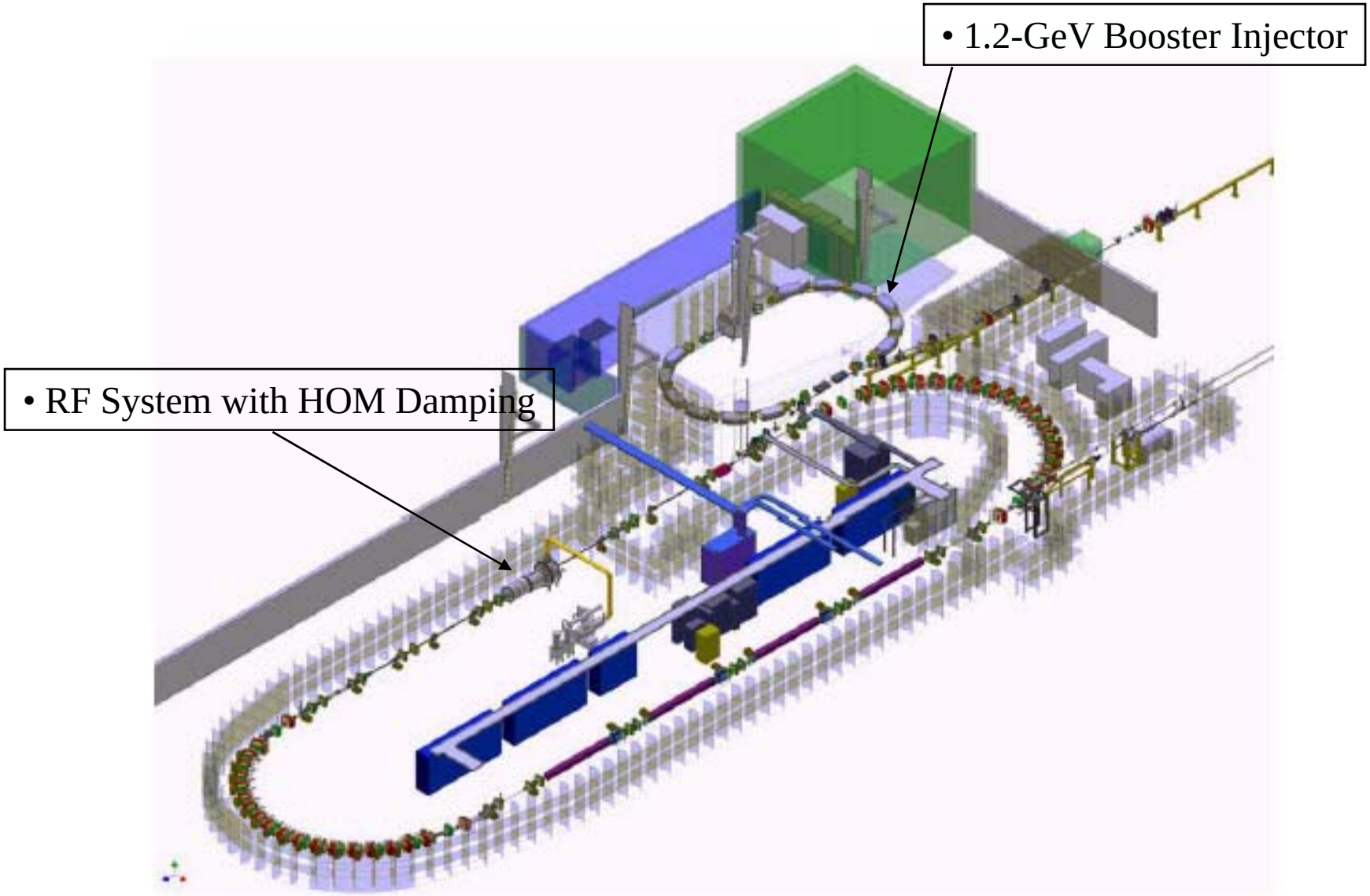

•Few-Body Physics @ HIγS

- Use the intense polarized beams at HIγS to perform double polarization experiments on 2, 3 (and 4) body systems.

- ***Resolve long standing cross section problems.***
- ***Measure fundamental properties such as nuclear polarizabilities.***
- ***Perform Precision tests of few-body theory including EFTs and 3-body force models.***
-

A recent low energy measurement of the fore-aft asymmetry in the d(γ,n)p reaction

Fore-Aft Asymmetry Measurement, a_s

⟶ A technique to study non-E1 radiation:

$$a_s = \frac{N_f - N_a}{N_f + N_a}$$

where N_f and N_a are the number of neutrons measured as the zeros of the Legendre polynomial P_2, the angles 54.7° and 125.3°. In terms of the Legendre polynomial expension of the cross section, the fore-aft asymmetry is written as :

$$a_s = \frac{0.5773 a_1 - 0.3849 a_3}{1 - 0.392 a_4}$$

The Experimental Setup

$E\gamma \longrightarrow$ 4.0, 3.5, 2.72, and 2.44 MeV

Linearly polarized, $\Delta E/E \sim 2$ %, I = 10^6 γ/s

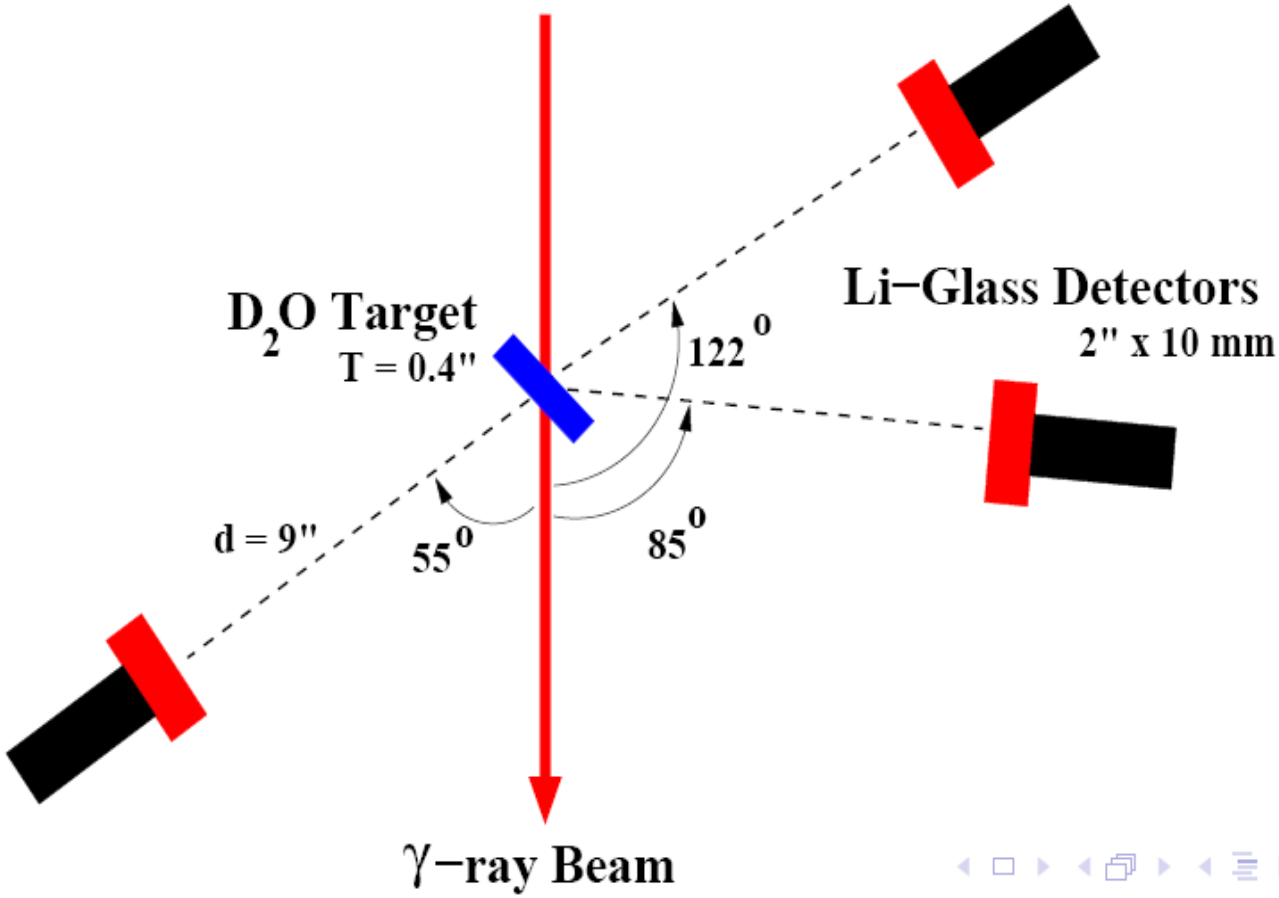

The Measurement : Fore-aft asymmetry (a_s), $d\sigma/d\Omega(\theta)$, and σ_T

- Time-of-Flight(ToF) $\longrightarrow$ The ToF is given by the time difference between the RF pulse of the accelerator and the Li-Glass detector signal.
- Energy $\longrightarrow$ Energy is measured by the pulse-height of the signal from the Li-Glass detector (Clear Signal $\rightarrow$ Due to ^{6}Li(n,α)T reaction (Q = 4.7 MeV), no threshold issues !).
- Analysis $\longrightarrow$ Number of counts in a detector are obtained by a sum of counts (in the region of interest) in ToF spectrum gated by the energy spectrum.

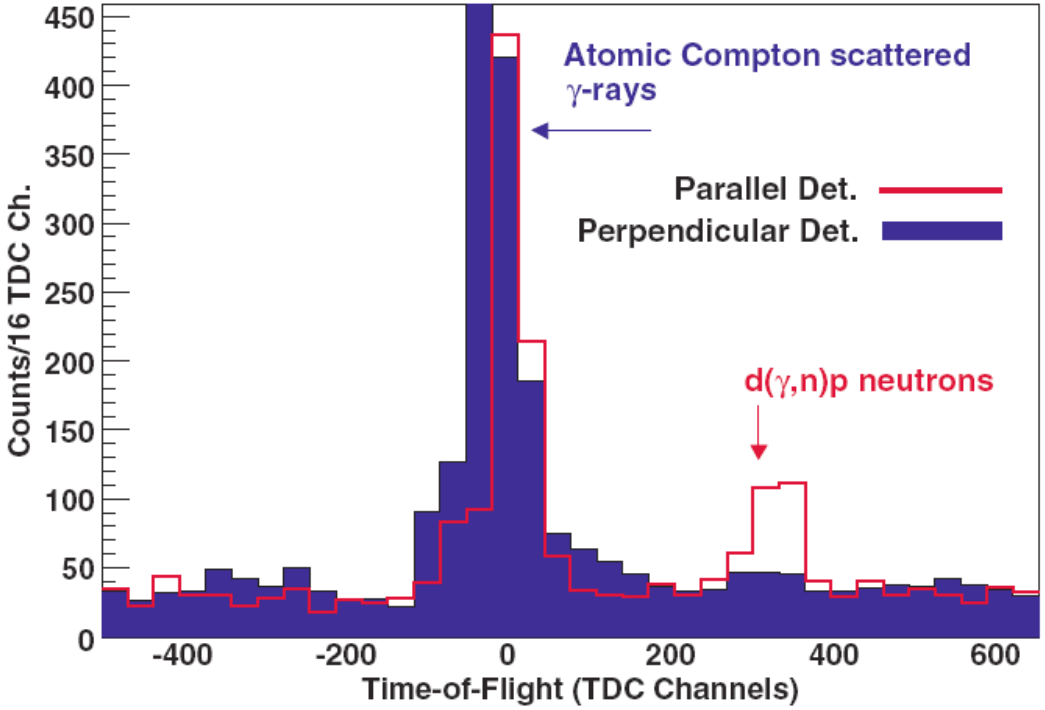

FIG. 2. (Color online) Time-of-Flight (ToF) spectrum from detectors parallel (open) and perpendicular (filled) to the γ-ray polarization axis. The energy of the γ rays was 2.72 MeV.

Why do we care about measuring a_s ?

An earlier experiment by Sawatzky *et al.*[4] reported a measurement of the a_1 coefficient to be 0.232 ± 0.07 and 0.1084 ± 0.039 at 3.5 and 4.0 MeV, respectively. This would indicate a significant E1-E2 interference, not predicted by any theory.

[4] Sawatzky, Brad, PhD thesis, UVa, 2005, and DNP02, DNP03

This Experiment : $\longrightarrow$ no significant d-waves

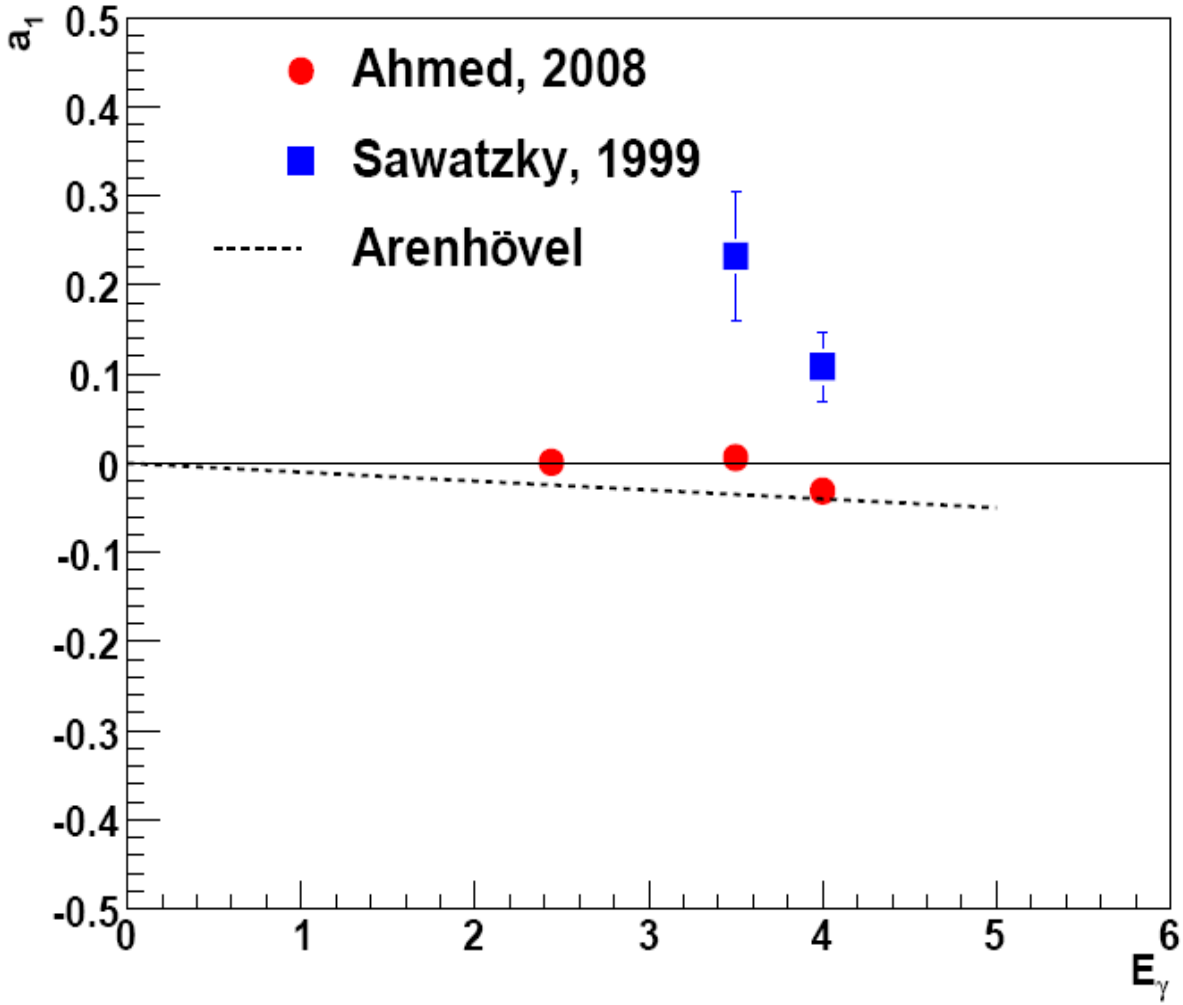

The differential cross section

At each energy, the measured yield at 90°(CoM) was normalized to the theoretical prediction by Arenhövel[5].

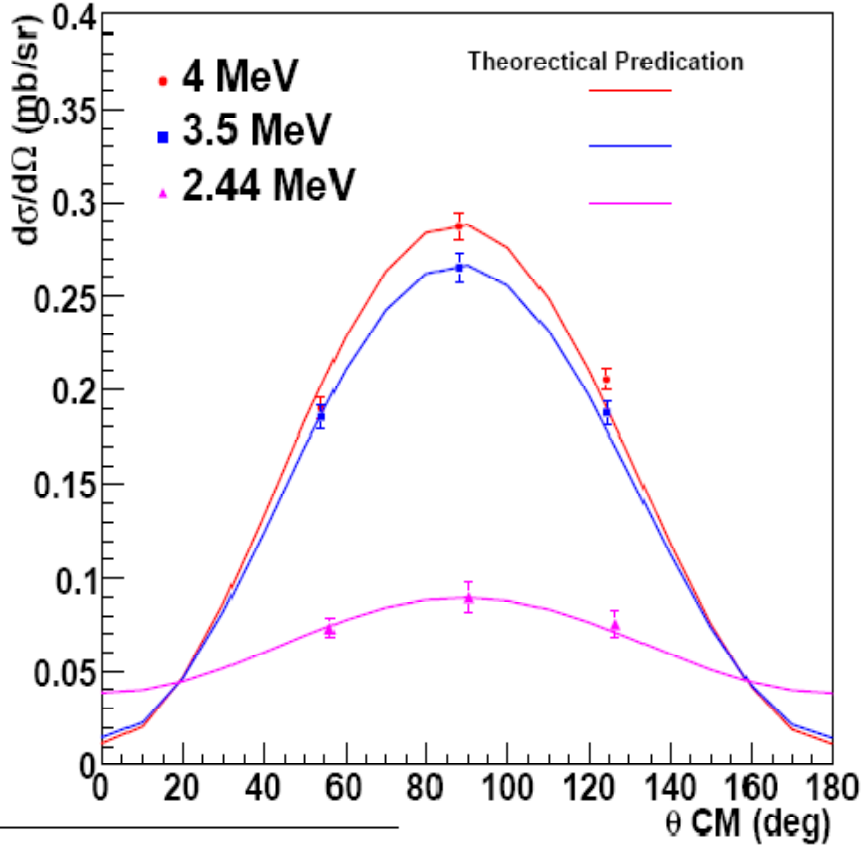

[5] H. Arenhövel, Few-Body Systems Suppl. 3 (1991)

The total cross section

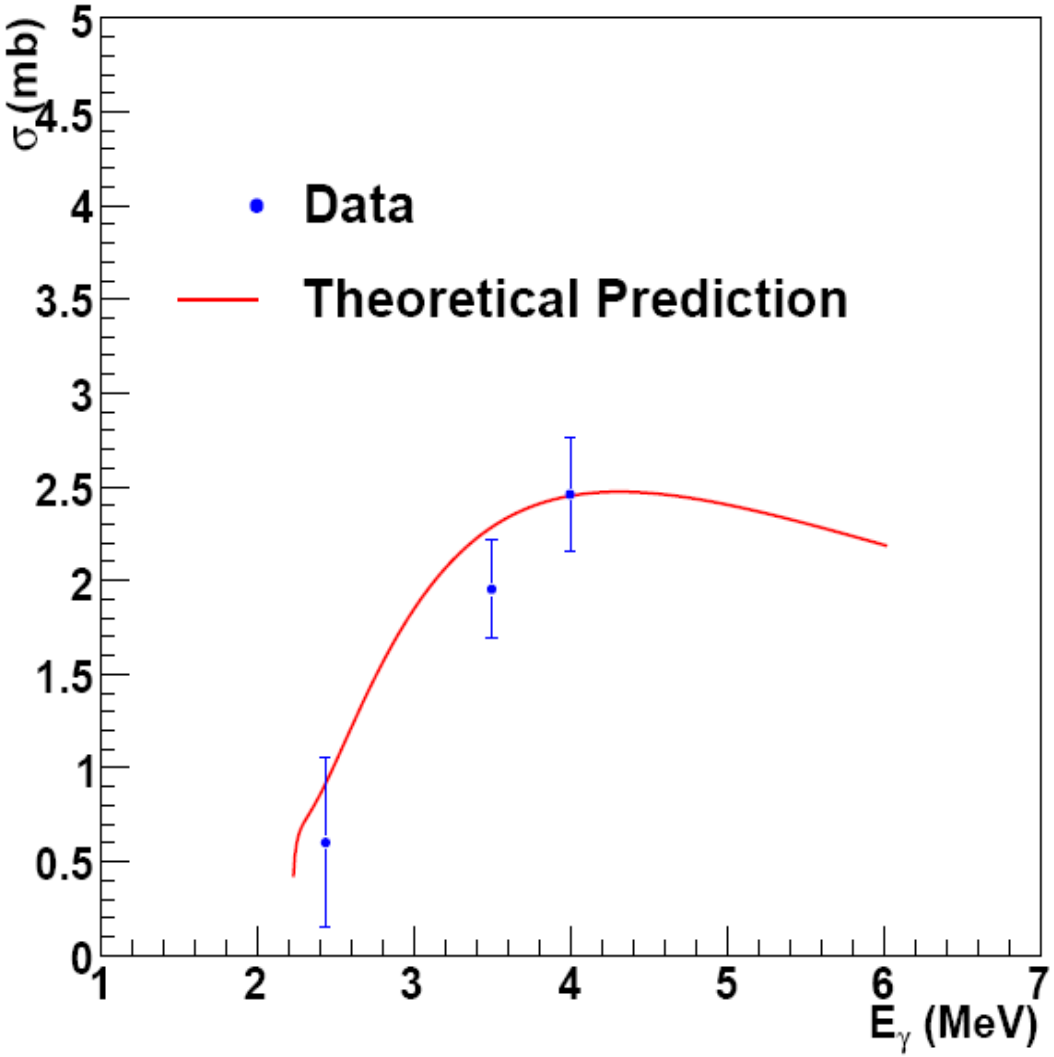

GDH Sum Rule studies @ HIγS

Measure the GDH integrand on d and ^{3}He below pion threshold.

- ***Compare to theoretical predictions. Provides extremely sensitive test of spin dependent effects such as relativistic spin-orbit currents.***
- ***Combine with the global effort to measure this for n, p and d. Our piece is essential for a test of consistency and a search for new physics.***

The Gerasimov-Drell-Hearn (GDH) Sum Rule for Deuteron

The GDH Integral

$$I^{GDH} = \int_{2.2\ \mathrm{MeV}}^{\infty} (\sigma_P(E) - \sigma_A(E)) \frac{dE}{E} = 4\,\pi^2\,\kappa^2\,\frac{e^2}{M^2}$$

$$\vec{M} = (Q+\kappa)\frac{e}{M}\vec{S};$$

$\sigma_{P/A}(E)$ are the total cross sections for the absorption of circularly polarized photons on a target with spin Parallel/Antiparallel to the spin of the photon;

κ = anomalous magnetic moment (of the deuteron).

$\kappa_d = -0.143\ \mu_m$ ⟶ I^{GDH} Predicted = 0.65 μb

$$I^{GDH}_{total} = \int_{2.2\ \mathrm{MeV}}^{E_\pi} \ldots + \int_{E_\pi}^{\infty} \ldots$$

E_π = pion production threshold

$$\int_{E_\pi}^{\infty} = \int (\text{proton}) + \int (\text{neutron})$$

$$= 436\ \mu b$$

$$\int_{2.2\ \mathrm{MeV}}^{E_\pi} \ldots \approx -436\ \mu b$$

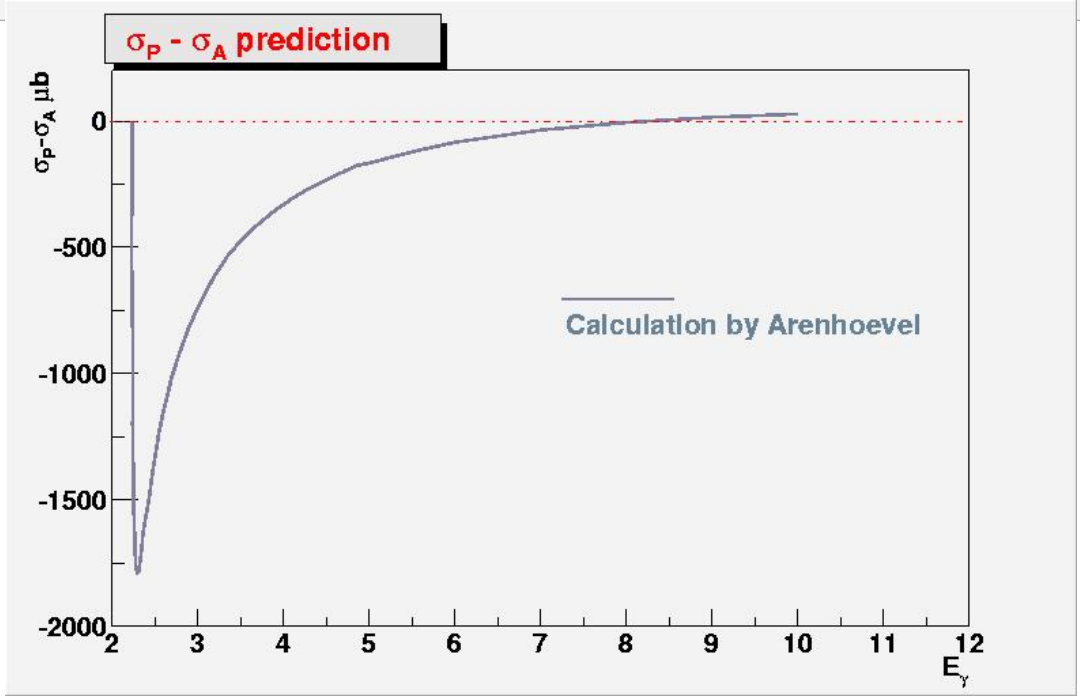

•THE GDH INTEGRAND FOR THE DEUTERON NEAR PHOTODISINTEGRATION THRESHOLD

• Contributions are expected from s-waves and p-waves (notation $^{2S+1}L_J$)

• M1 terms: $^1S_0$ and $^3S_1$
• Expect $^3S_1 \sim 0$.

• E1 terms: $^1P_1$, $^3P_0$, $^3P_1$, and $^3P_2$
• Expect the "spin-flip" E1 term $^1P_1 \sim 0$.

• Then→ $\sigma_P - \sigma_A = \pi/2k^2 \{ - {}^1S_0{}^2 - {}^3P_0{}^2 - 3/2\ {}^3P_1{}^2 + 5/2\ {}^3P_2{}^2 \}$

• If $^3P_0 \sim {}^3P_1 \sim {}^3P_2$

• Then $\sigma_P - \sigma_A = \pi/2k^2 \{ - {}^1S_0{}^2 \}$

• Which gives the result: $\sigma_P - \sigma_A$ **= -3 σ(M1)**

References to angular distribution formalism results for linear and circularly polarized gammas

Angular Distribution Coefficients for (γ,X) Reactions With Linearly Polarized Photons.

H. R. Weller et al.

At. Data and Nucl. Data Tables, Vol 50, No.1, Jan. 1992.

Angular Distribution Coefficients for (γ,X) Reactions With Circularly Polarized Photons and Polarized Target and a Correction to Previous Tables.

H. R. Weller et al.

At. Data and Nucl. Data Tables, Vol. 58, No.2, Nov. 1994.

Measurements of Σ(90º) were performed at 2.44, 2.60 and 2.72 MeV using four Li-glass detectors (Phys. Rev. C 77, 044005 (2008))

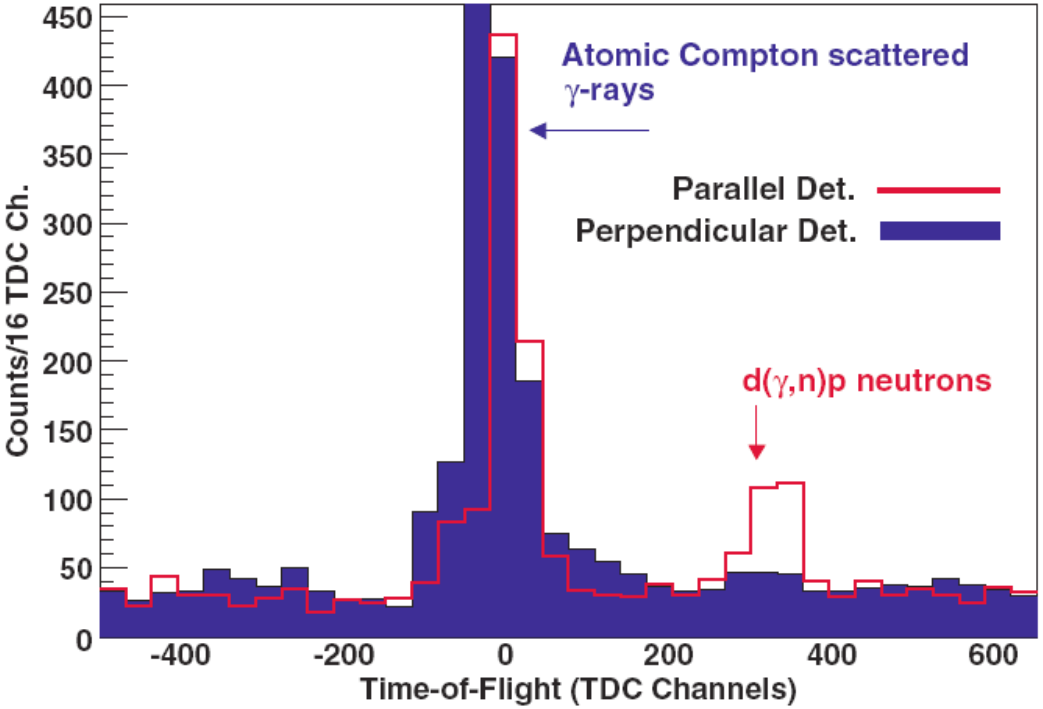

FIG. 2. (Color online) Time-of-Flight (ToF) spectrum from detectors parallel (open) and perpendicular (filled) to the γ-ray polarization axis. The energy of the γ rays was 2.72 MeV.

Extracting the fractional M1 contribution S(M1) from the measured analyzing power at 90°

$$\sigma(\theta,\phi) = \frac{\lambda\!\!\!^{-2}}{6}\left[\frac{1}{4}|S|^2 + \frac{27}{8}|P|^2\sin^2\theta(1+\cos 2\phi)\right]$$

$$\sigma(\theta,\phi) = R + \sin^2\theta(1+\cos 2\phi),$$

$$\tfrac{2}{27}|S|^2 = R|P|^2.$$

$$\Sigma(90^\circ) = \frac{1}{1+R}.$$

$$S(M1) = \frac{\frac{9}{4}R}{\frac{9}{4}R + \frac{3}{2}}.$$

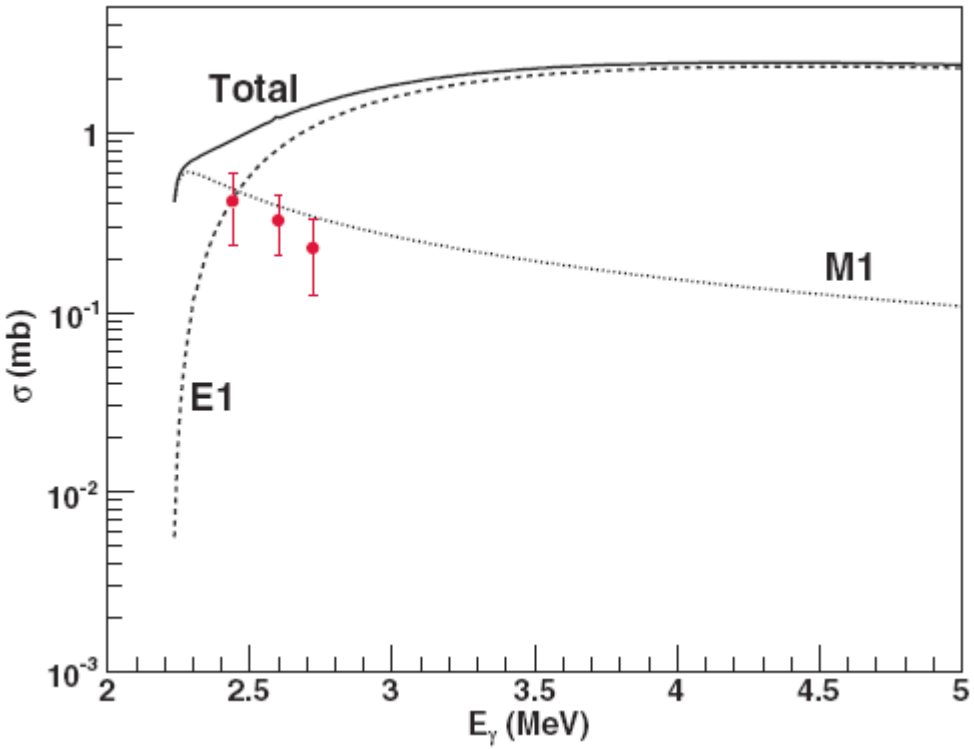
Total
M1
E1
σ (mb)
1
10^-1
10^-2
10^-3
2
2.5
3
3.5
4
4.5
5
Eγ (MeV)

$$\sigma_P - \sigma_A = \frac{\pi\lambda^2}{2}[-|M1(^1S_0)|^2]$$
$$= -3\sigma(M1).$$

We can also obtain the fractional M1 strength from polarized n-p capture or unpolarized d(γ,n)p if the polarization of the neutron is measured. The phase difference can be obtained from n-p scattering data.

$$A_y(90^\circ) = \frac{3|P||S|\sin(\phi_S - \phi_P)}{1 + \frac{9}{2}P^2},$$

with

$$9|P|^2 + |S|^2 = 1.0.$$

Obtaining a point near threshold from thermal neutron capture data

Thermal neutron capture cross section is well measured and known to be pure M1.

$$\sigma_{cap} = 332 \text{ +/- } 0.60 \text{ mb @ } E_n \sim 0.025 \text{ eV.}$$

The detailed balance factor is 1.6×10^{-6} giving

$$\sigma(M1) = 0.547\ \mu b \text{ @ } E_g = 2.2246 \text{ MeV.}$$

Using $\sigma_P - \sigma_A = -3\ \sigma(M1)$ gives

$$\boldsymbol{\sigma_P - \sigma_A = -1.641 \text{ +/- } 0.003\ \mu b \text{ @ } 2.2246 \text{ MeV}}$$

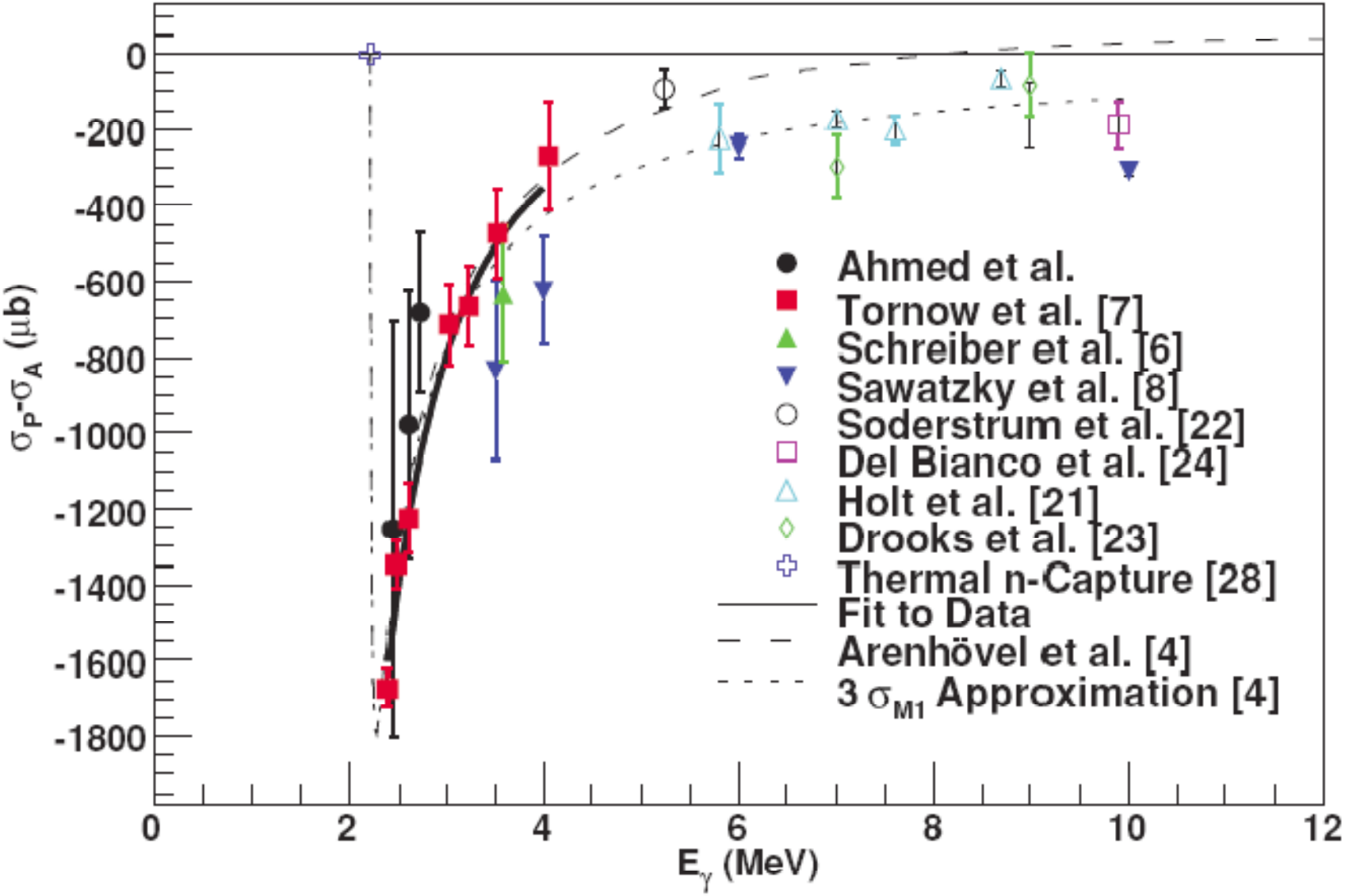
0
-200
-400
-600
-800
-1000
-1200
-1400
-1600
-1800
σ_P-σ_A (μb)
0
2
4
6
8
10
12
E_γ (MeV)
Ahmed et al.
Tornow et al. [7]
Schreiber et al. [6]
Sawatzky et al. [8]
Soderstrum et al. [22]
Del Bianco et al. [24]
Holt et al. [21]
Drooks et al. [23]
Thermal n-Capture [28]
Fit to Data
Arenhövel et al. [4]
3 σ_{M1} Approximation [4]

Results for the GDH integral at low energies

The solid black curve was a fit to the data using a Lorentzian line shape parameterized by amplitude, centroid and width. The GDH integral of this function up to 6 MeV gave a value of

GDH (thresh→6 MeV)$_{exp}$ = **-603 +/- 43 μb**

(note: already much larger than -436)

Theory (Arenhoevel et al.) gives **-627 μb (full)**

and **-662 μb (s-wave only)**

A second “sum-rule” which can be extracted is the forward spin polarizability γ_0

$$\gamma_0 = -\frac{1}{8\pi^2}\int_{\omega_{\rm th}}^{\infty}(\sigma_P(\omega)-\sigma_A(\omega))\frac{d\omega}{\omega^3}.$$

Xiangdong Ji and Yingchuan Li have calculated the forward spin polarizability of the deuteron to next-to-leading order in pionless EFT.
(Phys. Letts. B 591 (2004) 76 -82)
(determined by deut BE, isovector nucl. mag. mom., $^1S_0$ scatt length)

$$\gamma^{\mathrm{LO}} = \frac{\alpha_{\mathrm{em}}(\mu^{(1)})^2}{16\gamma^4}\left[1 + \frac{M_N\gamma}{2\pi}\mathcal{A}_{-1}^{(^1S_0)}(-B) \times \left(1 + \frac{M_N\gamma}{4\pi}\mathcal{A}_{-1}^{(^1S_0)}(-B)\right)\right] + \frac{\alpha_{\mathrm{em}}(4\mu^{(1)} - 1)}{128\gamma^4}. \quad (30)$$

The numerical value of γ at this order is 3.762 fm^4.

At the next-to-leading order, there are contributions from the C_2 coupling in the singlet and triplet channels

where

$$C_2^{(^1S_0)}(\mu) = \frac{4\pi}{M_N}\frac{r_0}{2}\frac{1}{(\mu - 1/a^{(^1S_0)})^2},$$

$$C_2^{(^3S_1)}(\mu) = \frac{2\pi}{M_N}\frac{\rho_d}{(\mu - \gamma)^2}, \tag{32}$$

with $r_0 = 2.73$ fm. There are also contributions from the following electromagnetic counter term [17]

$$\mathcal{L}'' = eL_1\left(N^T P_i N\right)^\dagger\left(N^T \bar{P}_3 N\right)B_i. \tag{33}$$

Using the counter term determined from the neutron capture, $L_1(m_\pi) = 7.24\ \mathrm{fm}^4$ [3], we find $\gamma^{\mathrm{NLO}} = 0.50\ \mathrm{fm}^4$ which is about 10% of the leading-order result. Therefore the effective field theory expansion seems to converge well.

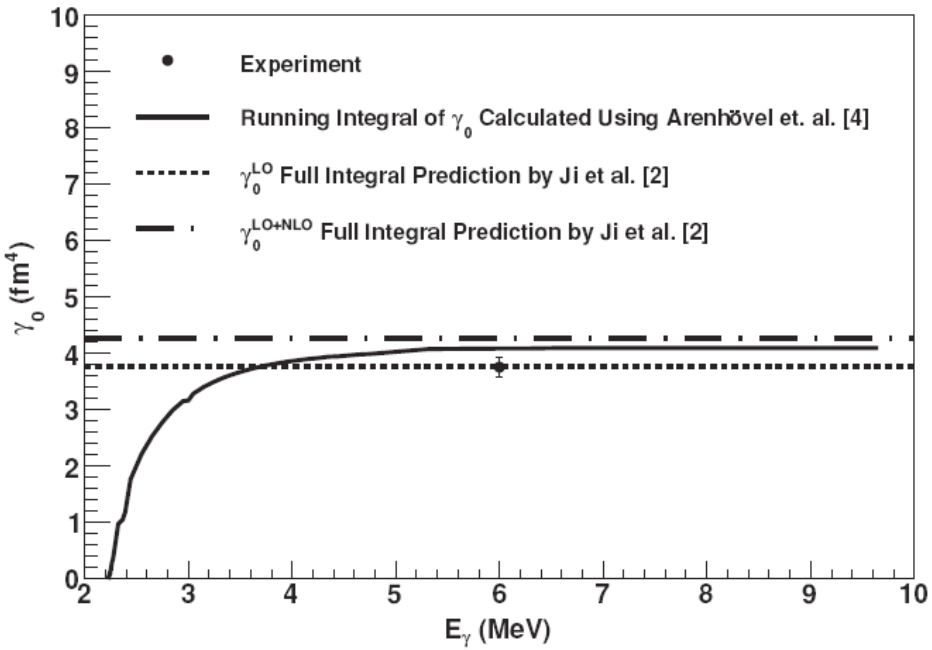

FIG. 6. Running integral of γ_0 calculated using σ_P-σ_A predictions of Arenhövel *et al.* [12]. Also shown are the values of the full integral predictions of Ji *et al.* [2] for γ_0^{LO} and $\gamma_0^{\mathrm{LO+NLO}}$. The predictions are compared to the experimental result integrated up to 6 MeV.

Predicted behavior (Ahrenhovel) of the GDH integrand. Solid line includes a *relativisitic* correction.

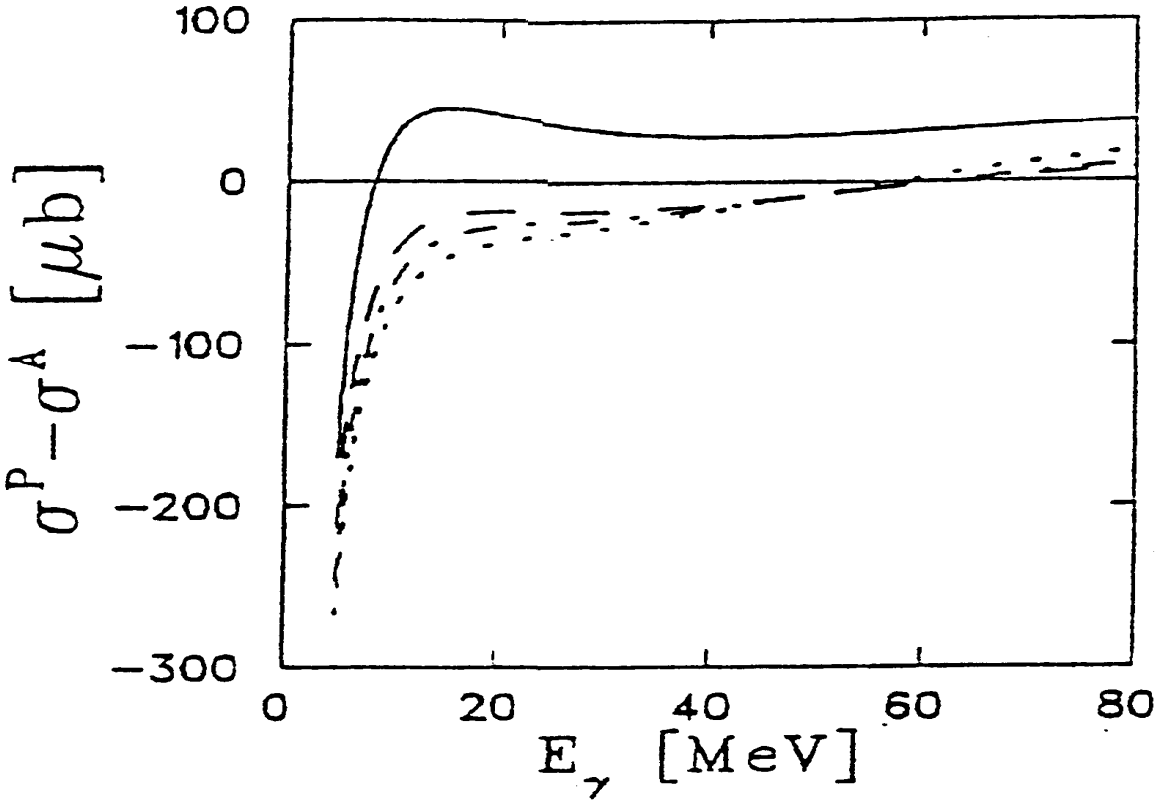

Relativistic contributions

Leading order relativistic contributions are required to give the correct form of the term linear in photon momentum in the low-energy expansion of the Compton amplitude.

The relativistic spin-orbit current effects the splitting of the p-wave amplitudes, leading to a positive value of the GDH integrand. (*It increases the relative strength of the* $^3p_2$ *term.)*

$$\sigma_P - \sigma_A = \frac{\pi \lambda\!\!\!^{-2}}{2}\Big[- |M1(^1S_0)|^2 - |E1(^3P_0)|^2 - \frac{3}{2}|E1(^3P_1)|^2 + \frac{5}{2}|E1(^3P_2)|^2 - \frac{3}{2}|E2(^3D_1)|^2 - \frac{5}{6}|E2(^3D_2)|^2 + \frac{7}{3}|E2(^3D_3)|^2 \Big], \tag{9}$$

d(γ,n)p at 14 and 16 MeV

(Dissertation topic of Dr. Matthew Blackston)

Used the 88 neutron detector array Blowfish (had TOF and PSD).

Heavy water target.

100% linearly polarized beams.

A full simulation was performed using Geant4 to correct the data for finite geometry and multiple scattering effects.

The upgraded *BLOWFISH array*

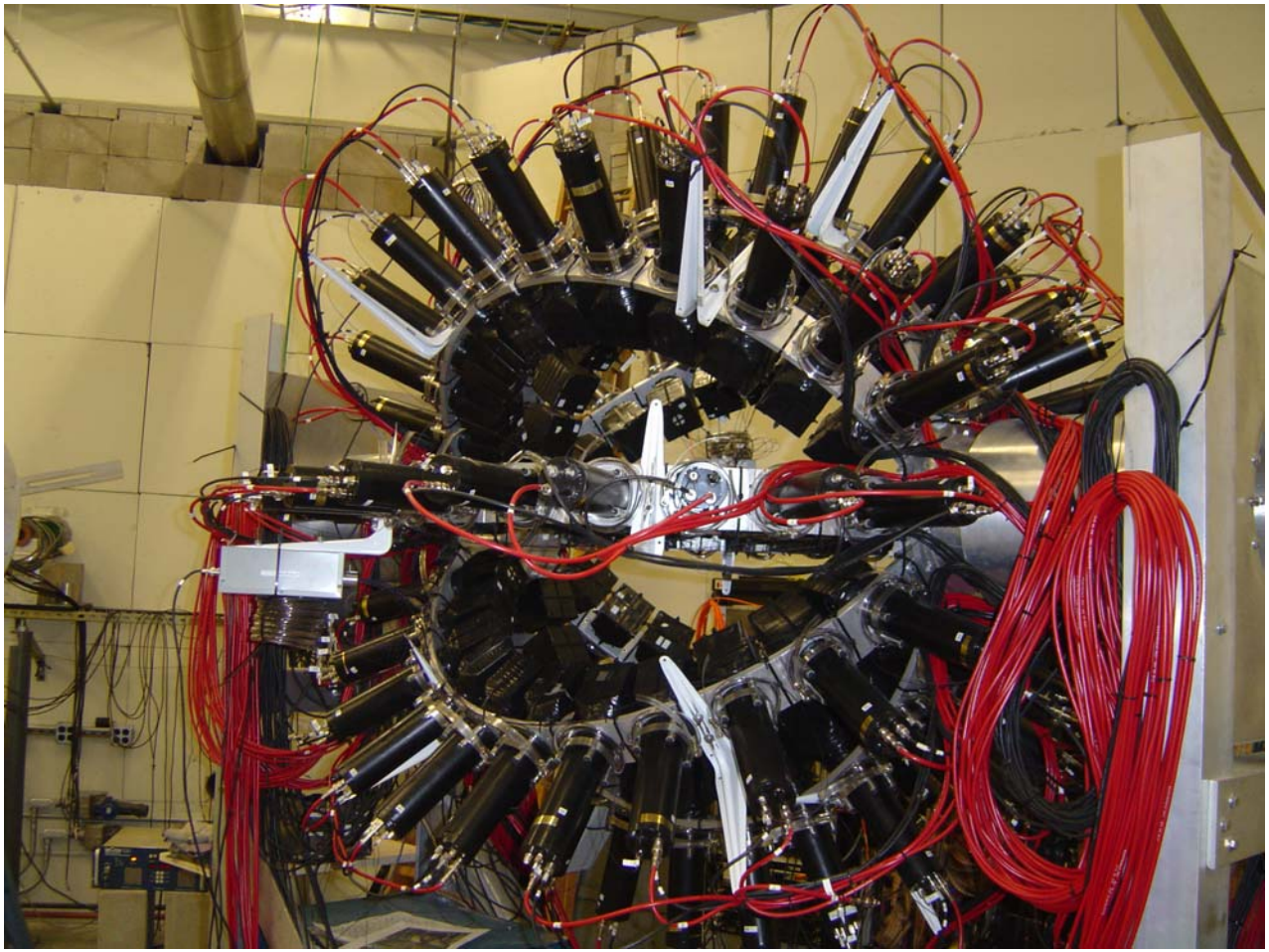

- Expansion of $\sigma(\theta)$ and $\Sigma(\theta)$ in Terms of Legendre Polynomials

$$\sigma(\theta) = a_0 \left[1 + \sum_{k=1} a_k P_k(cos\ \theta) \right] \qquad \Sigma(\theta)\sigma(\theta) = \sum_{k=2} e_k P_k^2(cos\ \theta)$$

- Using the Formalism of Weller *et al.*[2], a_k's and e_k's can be expanded in terms of amplitudes and relative phases of the Reduced Transition Matrix Elements (TMEs)

References to angular distribution formalism results for linear and circularly polarized gammas

Angular Distribution Coefficients for (γ,X) Reactions With Linearly Polarized Photons.

H. R. Weller et al.

At. Data and Nucl. Data Tables, Vol 50, No.1, Jan. 1992.

Angular Distribution Coefficients for (γ,X) Reactions With Circularly Polarized Photons and Polarized Target and a Correction to Previous Tables.

H. R. Weller et al.

At. Data and Nucl. Data Tables, Vol. 58, No.2, Nov. 1994.

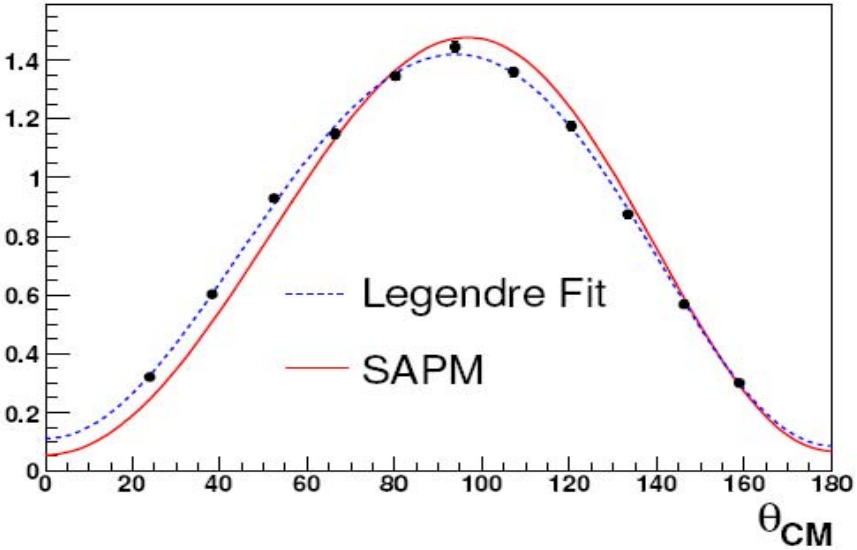

(a) 14 MeV Unpolarized Cross Section.

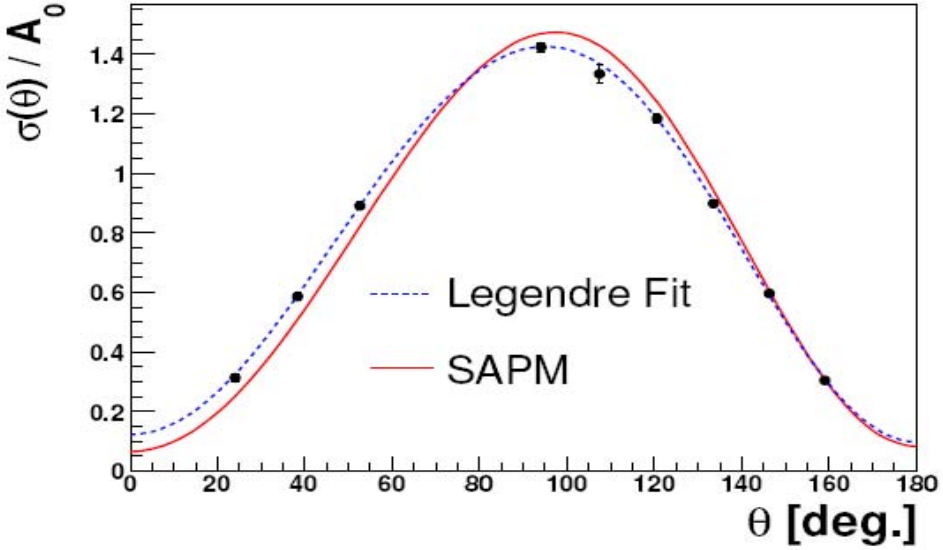

(b) 16 MeV Unpolarized Cross Section.

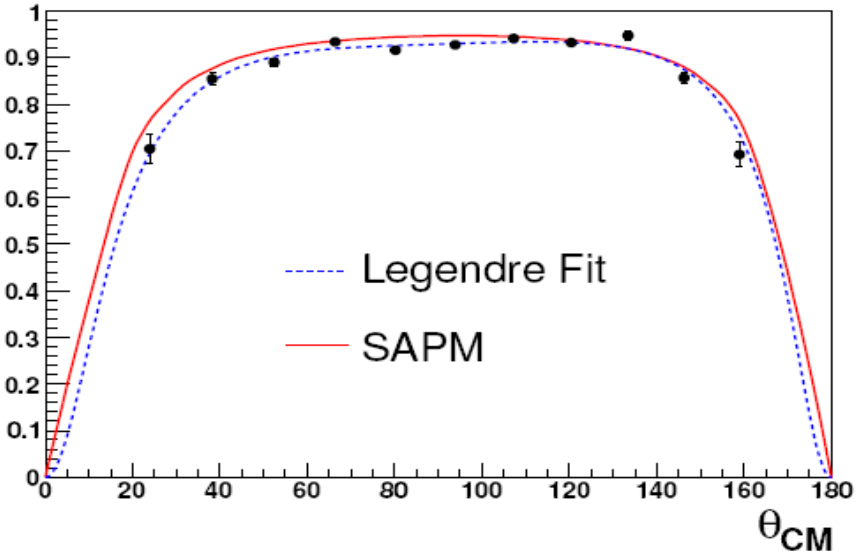

(c) 14 MeV Analyzing Power.

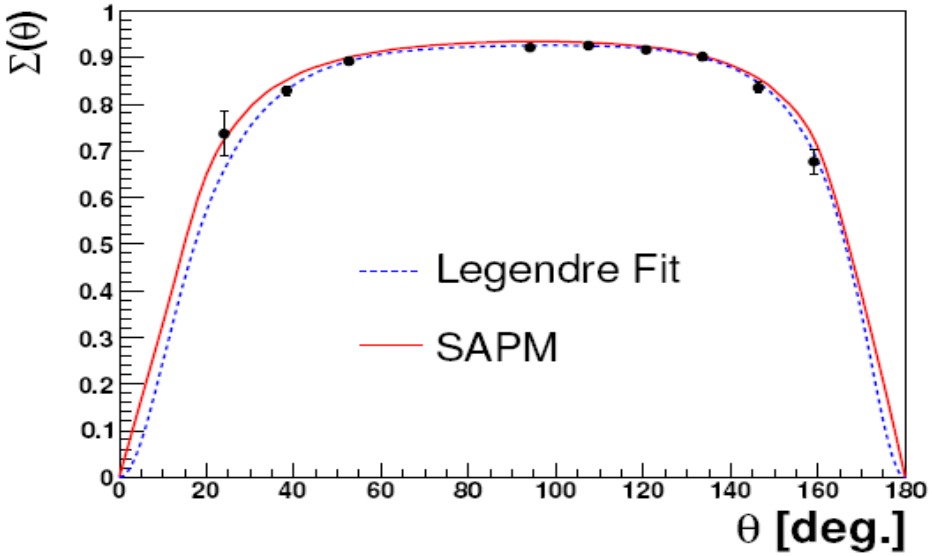

(d) 16 MeV Analyzing Power.

Fitting Functions

$$a_0 = 0.25|s|^2 + 2.25|p|^2 + 3.75|d|^2 \equiv 1$$

$$a_1 = 7.794\ |p||d|cos(\delta_{pd})$$

$$a_2 = -2.25|p|^2 + 2.678|d|^2 \qquad e_2 = \tfrac{1}{2}(2.25|p|^2 + 2.678|d|^2)$$

$$a_3 = -7.794|p||d|cos(\delta_{pd}) \qquad e_3 = \tfrac{1}{6}(7.794|p||d|cos(\delta_{pd}))$$

$$a_4 = -6.429|d|^2 \qquad e_4 = \tfrac{1}{12}(6.429|d|^2)$$

- Watson's Theorem[3] - use *n*-*p* scattering phase shifts to fix δ_{pd}
- SAID[4] gives $\delta_{pd} \sim 1^\circ$ for each energy

[3] L. D. Knutson, Phys. Rev. **C59**(1999) 2152
[4] SAID analysis, Center for Nuclear Studies, The George Washington University

Constraints

There are four constraint relationships in these equations:

$e_2 = - ½ a_2$

$e_3 = - 1/6 a_3$

$e_4 = - 1/12 a_4$

$a_1 = - a_3$

Two of these survive in the full equations

$e_3 = - 1/6 a_3$; and $e_4 = - 1/12 a_4$. We therefore have six linearly independent knowns. Since there are seven amplitudes, we fixed the s-wave value to theory, and fit the data to determine the 3 p-wave and the 3 d-wave terms.

$$
\begin{aligned}
A_0 &= 0.25\ |^1s_0(M1)|^2 + 0.25\ |^3p_0(E1)|^2 + 0.75\ |^3p_1(E1)|^2 \\
&+ 1.25\ |^3p_2(E1)|^2 + 0.75\ |^3d_1(E2)|^2 + 1.25\ |^3d_2(E2)|^2 \\
&+ 1.75\ |^3d_3(E2)|^2
\end{aligned} \tag{A.1}
$$

$$
\begin{aligned}
a_1 &= 0.866\ |^3p_0(E1)|\ |^3d_1(E2)|\ cos(\delta_{^3p_0} - \delta_{^3d_1}) \\
&+ 0.649\ |^3p_1(E1)|\ |^3d_1(E2)|\ cos(\delta_{^3p_1} - \delta_{^3d_1}) \\
&+ 1.949\ |^3p_1(E1)|\ |^3d_2(E2)|\ cos(\delta_{^3p_1} - \delta_{^3d_2}) \\
&+ 0.043\ |^3p_2(E1)|\ |^3d_1(E2)|\ cos(\delta_{^3p_2} - \delta_{^3d_1}) \\
&+ 0.649\ |^3d_2(E2)|\ |^3p_2(E1)|\ cos(\delta_{^3d_2} - \delta_{^3p_2}) \\
&+ 3.637\ |^3p_2(E1)|\ |^3d_3(E2)|\ cos(\delta_{^3p_2} - \delta_{^3d_3})
\end{aligned} \tag{A.2}
$$

$$
\begin{aligned}
a_2 &= -0.187\ |^3p_1(E1)|^2 \\
&- 0.438\ |^3p_2(E1)|^2 + 0.187\ |^3d_1(E2)|^2 \\
&+ 0.223\ |^3d_2(E2)|^2 + 0.857\ |^3d_3(E2)|^2 \\
&- 0.500\ |^3p_0(E1)|\ |^3p_2(E1)|\ cos(\delta_{^3p_0} - \delta_{^3p_2}) \\
&- 1.125\ |^3p_1(E1)|\ |^3p_2(E1)|\ cos(\delta_{^3p_1} - \delta_{^3p_2}) \\
&+ 0.625\ |^3d_1(E2)|\ |^3d_2(E2)|\ cos(\delta_{^3d_1} - \delta_{^3d_2}) \\
&+ 0.071\ |^3d_1(E2)|\ |^3d_3(E2)|\ cos(\delta_{^3d_1} - \delta_{^3d_3}) \\
&+ 0.714\ |^3d_2(E2)|\ |^3d_3(E2)|\ cos(\delta_{^3d_2} - \delta_{^3d_3})
\end{aligned} \tag{A.3}
$$

$$
\begin{aligned}
a_3 &= -0.866\ |^3p_0(E1)|\ |^3d_3(E2)|\ cos(\delta_{^3p_0} - \delta_{^3d_3}) \\
&+ -1.732\ |^3p_1(E1)|\ |^3d_3(E2)|\ cos(\delta_{^3p_1} - \delta_{^3d_3}) \\
&+ -1.732\ |^3p_2(E1)|\ |^3d_2(E2)|\ cos(\delta_{^3p_2} - \delta_{^3d_2}) \\
&+ -1.559\ |^3p_2(E1)|\ |^3d_1(E2)|\ cos(\delta_{^3p_2} - \delta_{^3d_1}) \\
&+ -1.039\ |^3p_2(E1)|\ |^3d_3(E2)|\ cos(\delta_{^3p_2} - \delta_{^3d_3}) \\
&+ -0.866\ |^3d_2(E2)|\ |^3p_1(E1)|\ cos(\delta_{^3d_2} - \delta_{^3p_1})
\end{aligned}
$$

$$
\begin{aligned}
a_4 &= -0.952\ |^3d_2(E2)|^2 - 0.524\ |^3d_3(E2)|^2 \\
&+ -2.571\ |^3d_3(E2)|\ |^3d_1(E2)|\ cos(\delta_{^3d_3} - \delta_{^3d_1}) \\
&+ -2.381\ |^3d_2(E2)|\ |^3d_3(E2)|\ cos(\delta_{^3d_2} - \delta_{^3d_3})
\end{aligned}
$$

Phase shifts from the SAID n-p scattering analysis

For $E_\gamma = 14$ MeV (E_n (lab) = 23.6 MeV)

$^1S_0$	50.74^o
$^3P_0$	8.61^o
$^3P_1$	-4.88^o
$^3P_2$	2.86^o
$^3D_1$	-2.9^o
$^3D_2$	4.12^o
$^3D_3$	0.13^o

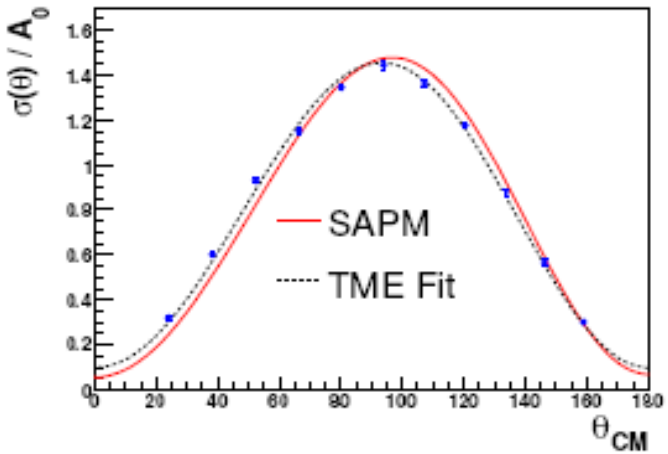

(a) 14 MeV Unpolarized Cross Section.

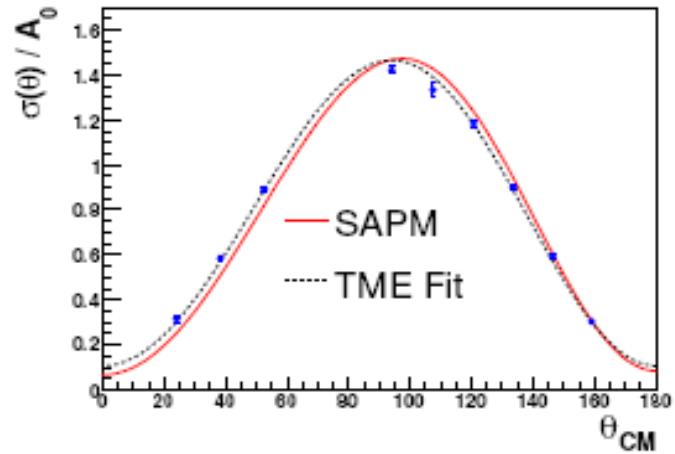

(b) 16 MeV Unpolarized Cross Section.

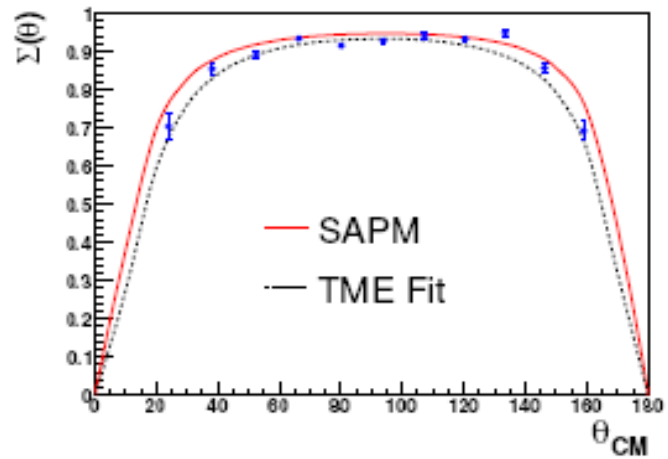

(c) 14 MeV Analyzing Power.

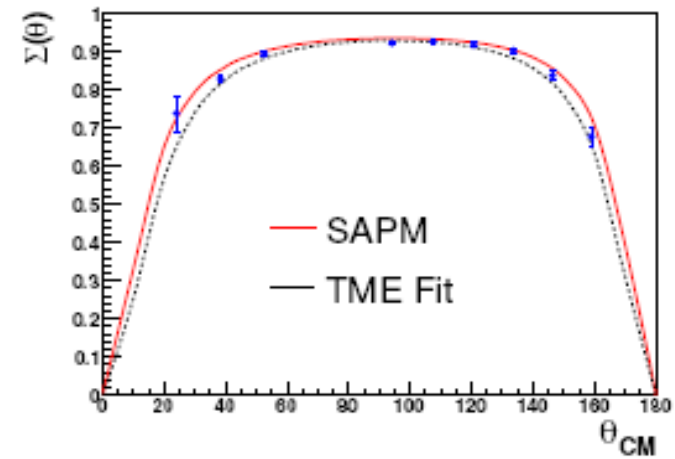

(d) 16 MeV Analyzing Power.

Figure 6.8: Fits to the observables with the assumption of no splittings. The error bars on the data are statistical only. The blue curve is the fit and the red curve is from the SAPM calculation.

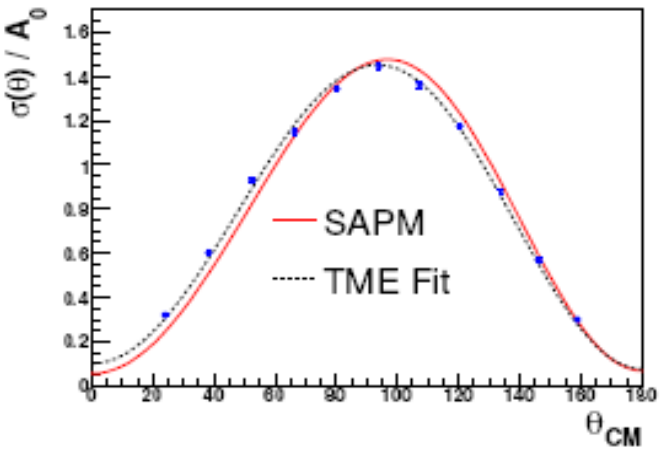

(a) 14 MeV Unpolarized Cross Section.

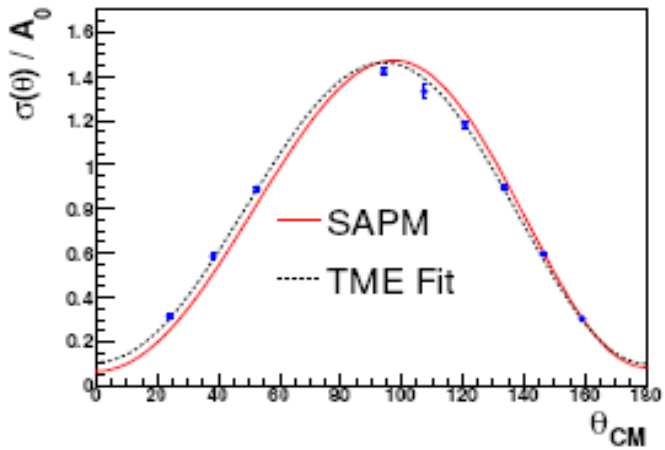

(b) 16 MeV Unpolarized Cross Section.

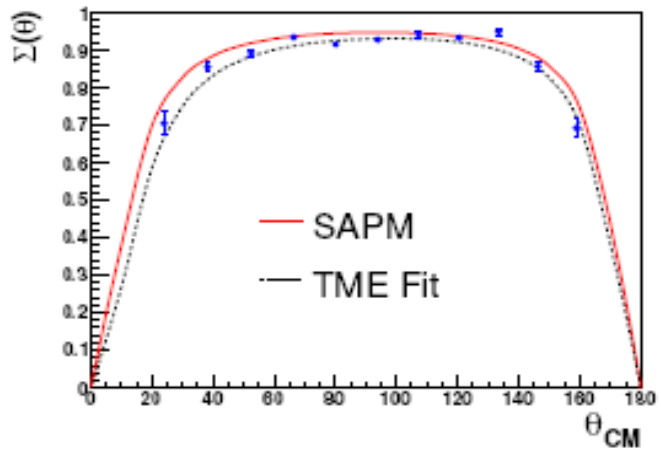

(c) 14 MeV Analyzing Power.

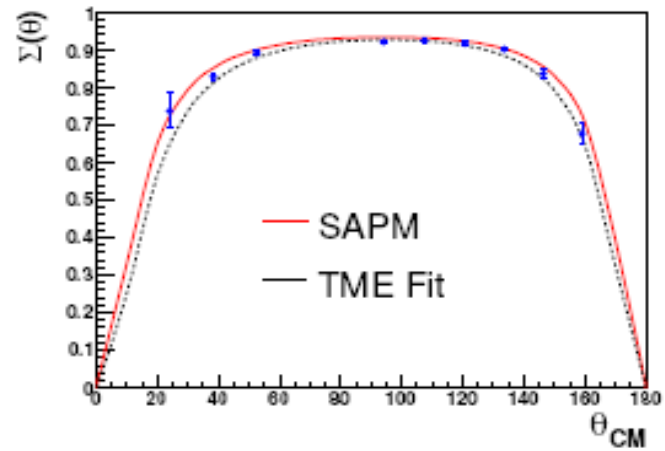

(d) 16 MeV Analyzing Power.

Figure 6.11: Fits to the observables with splittings. The error bars are statistical only. The blue curve is the fit and the red curve is from the SAPM calculation.

First determination of the splittings in the p-wave (E1) amplitudes in photodisintegration of the deuteron
14 MeV data set
(no splitting values: 0.42)

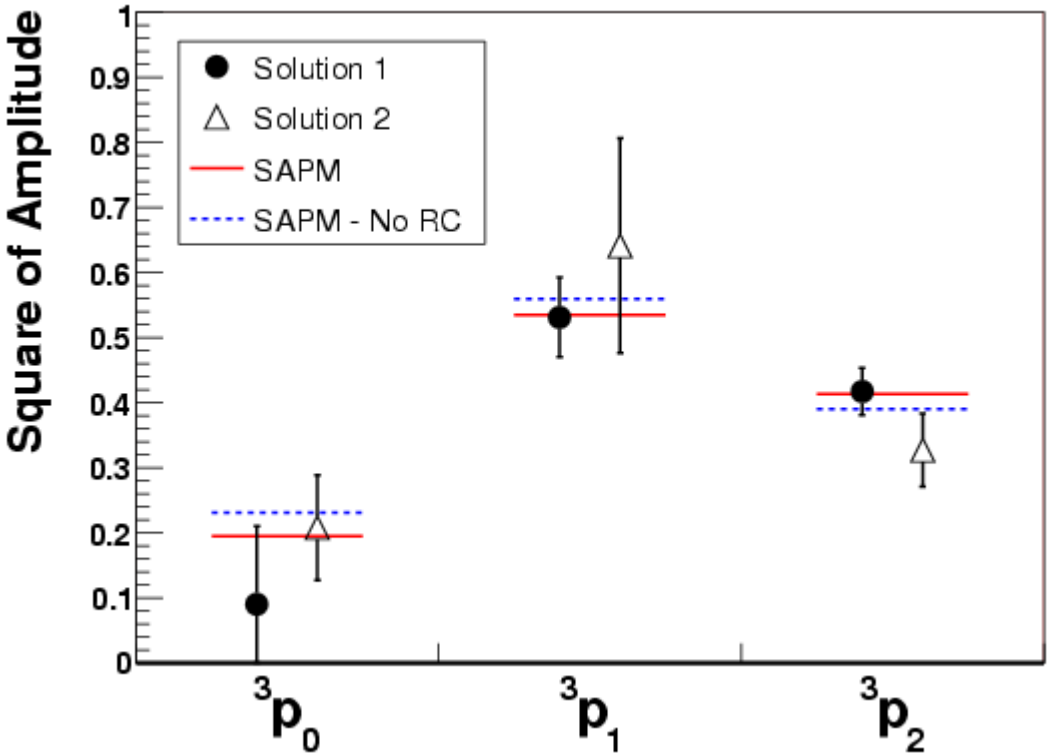

•First determination of the splittings in the p-wave (E1) amplitudes in photodisintegration of the deuteron at 16 MeV.

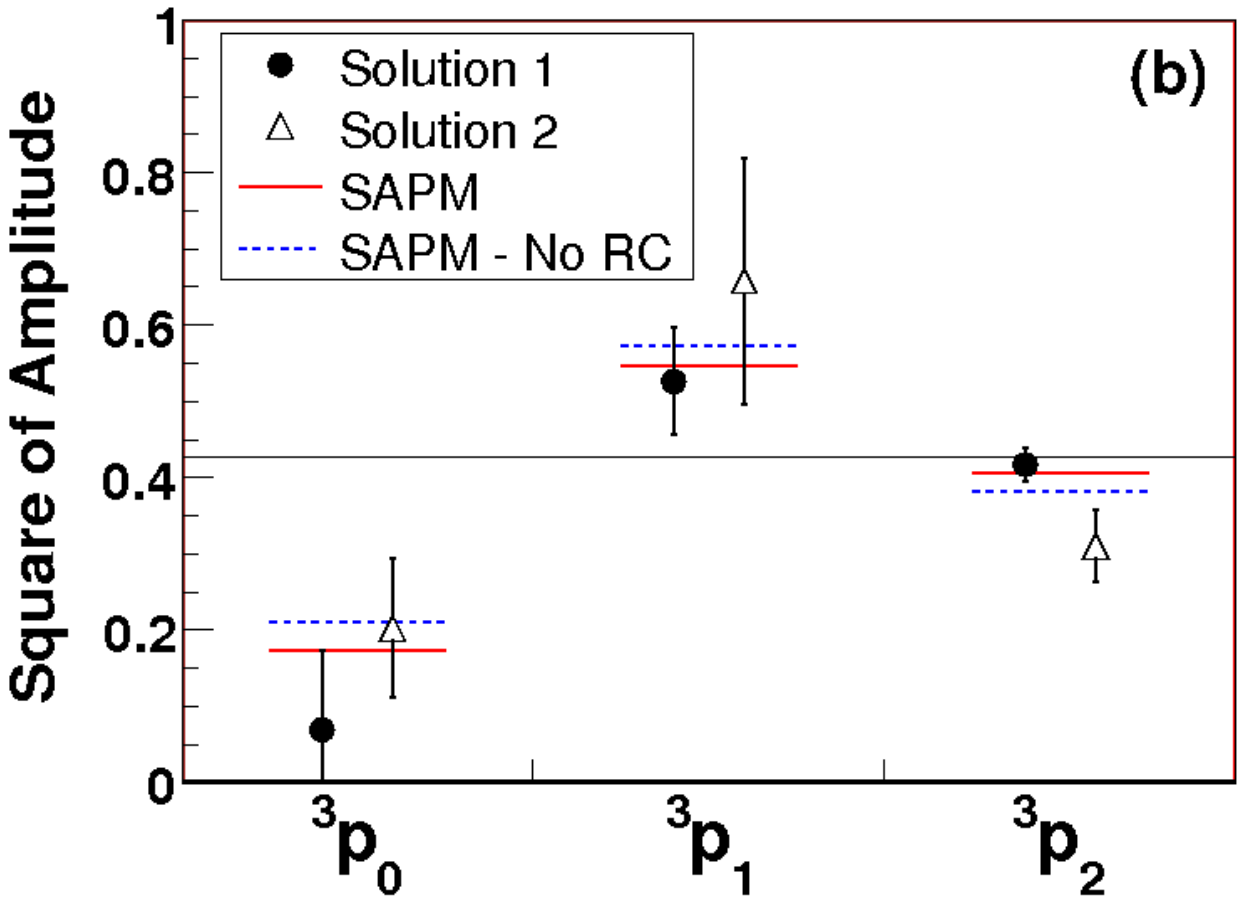

Results for the GDH integrand from the two solutions. Without p-wave splittings the value at 14 MeV is predicted to be -50 μb (from the s-wave M1 term). Positive values are predicted only when the relativistic contribution is included.

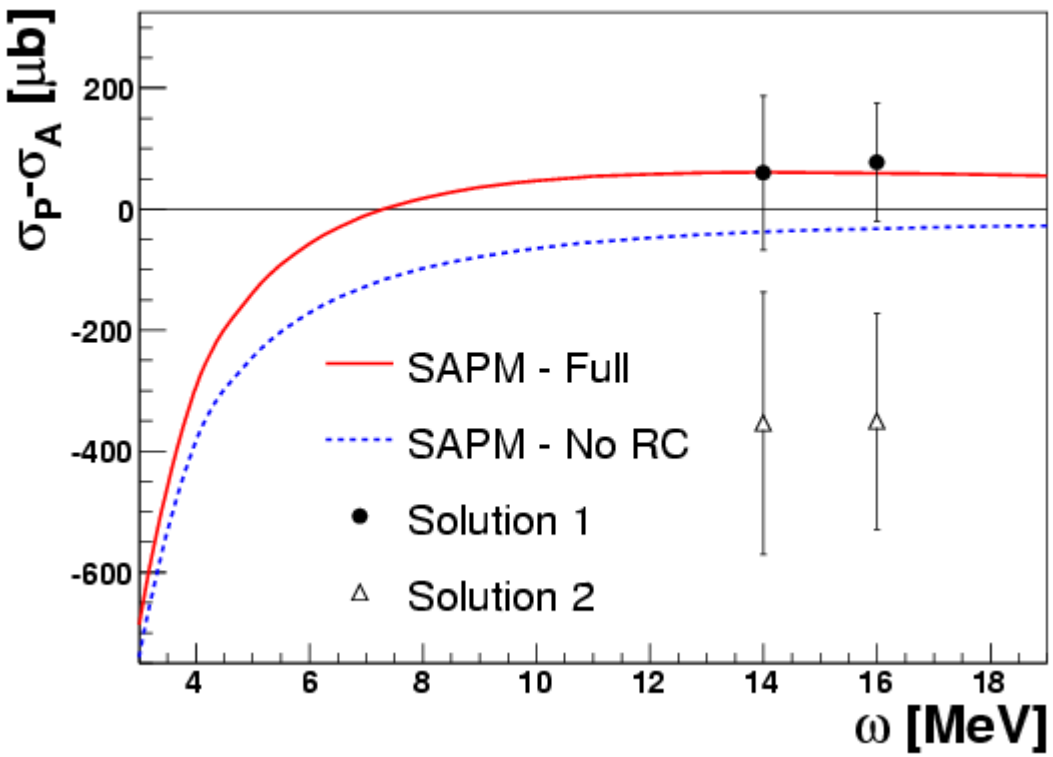

Requirements for measurements of
The GDH
integrand on the Deuteron

Circularly Polarized gamma rays—available NOW!

Neutron detection array—Blowfish *–ready to go!*

Polarized frozen-spin target—Under construction in collaboration with *Don Crabb* and *Blaine Norum* of U. Va. Scheduled to be installed this fall.

The upgraded *BLOWFISH array*

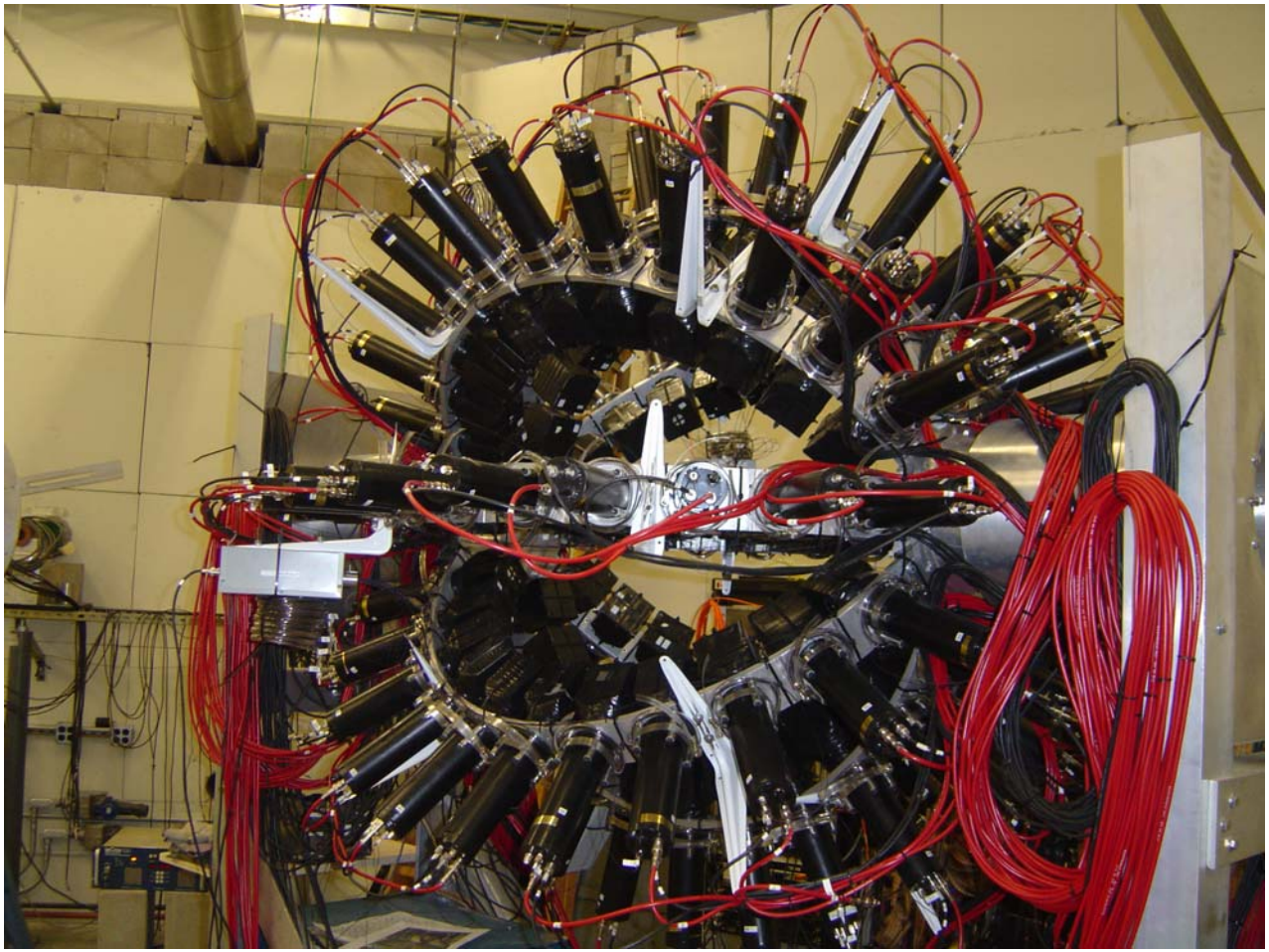

Frozen Spin Polarized Deuterium Target --target and installation (loading dock system) are *fully funded*.

- Butanol
- Polarization ~ 80 %
- Polarizing Field ~ 2.5 T

Holding Field ~ 0.6 T

Thickness ~ 3.5 x 10^{23} d/cm^2

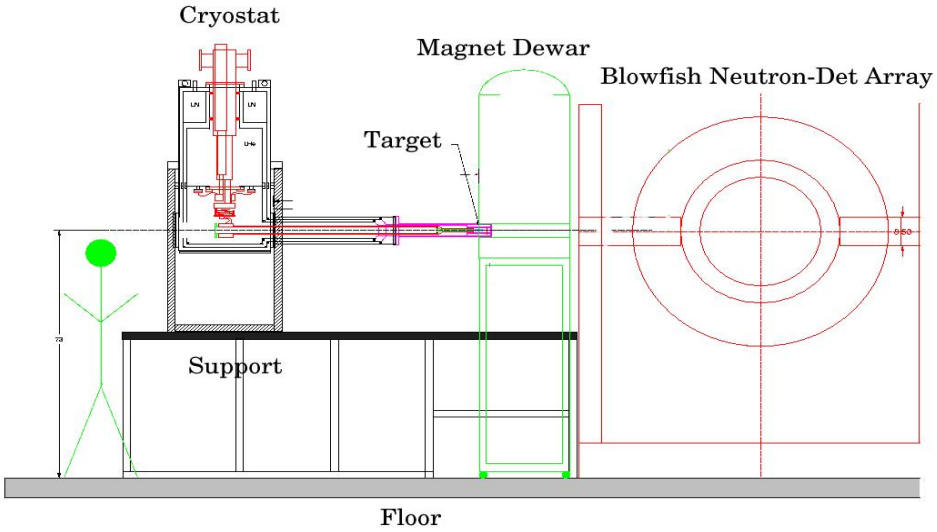

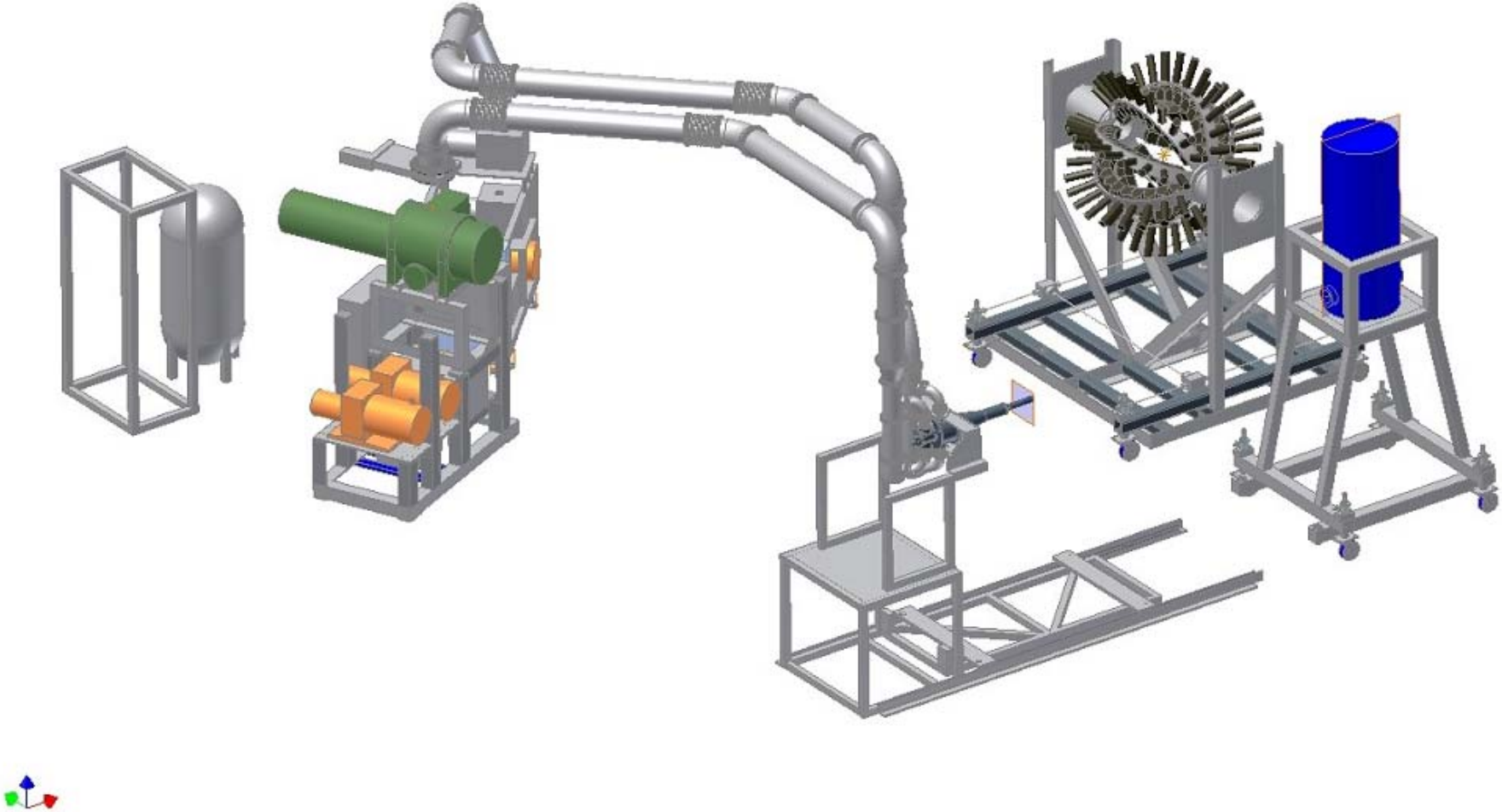

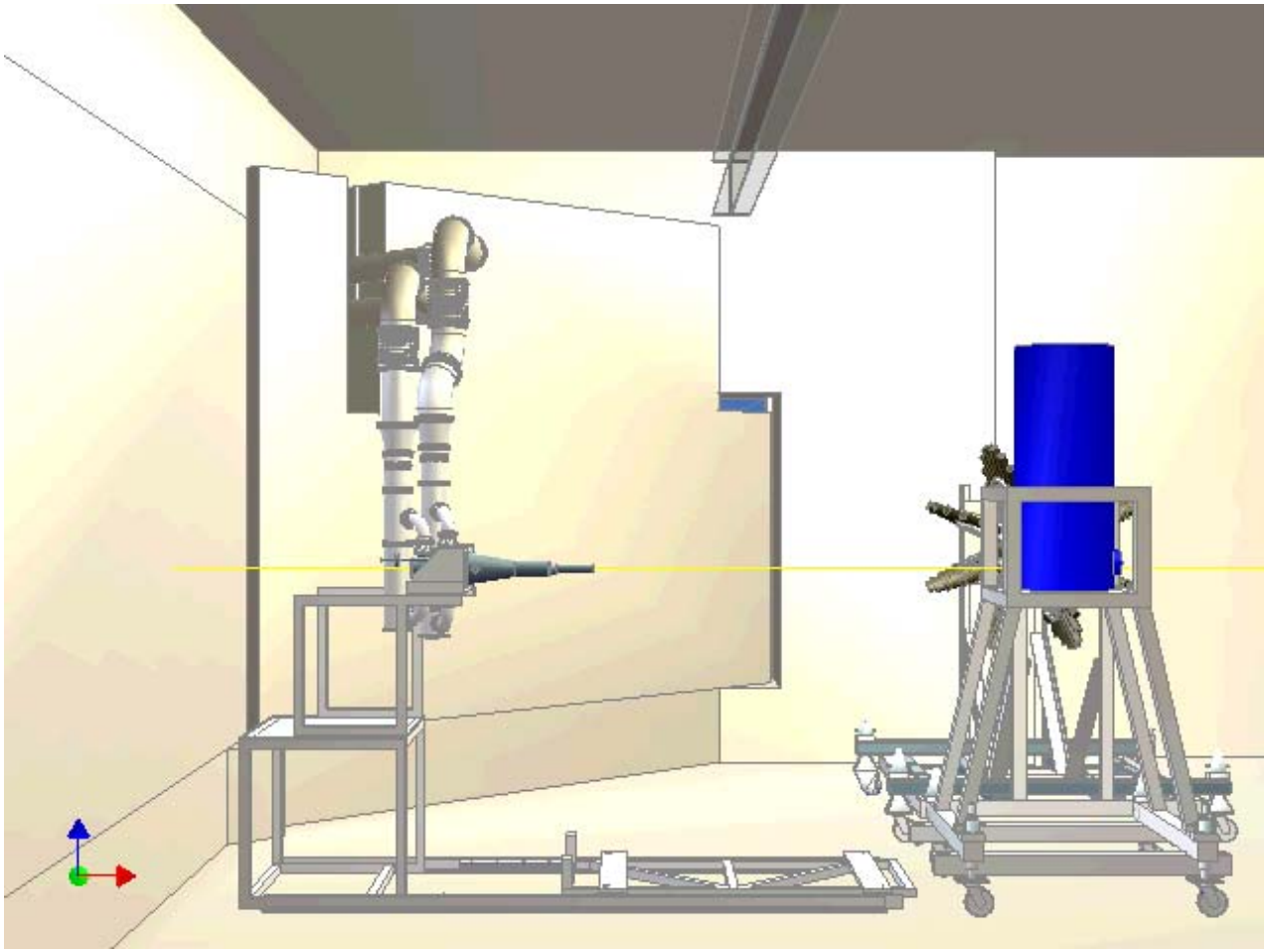

The GDH integrand for deuterium

A 300 hour run will allow us to measure the GDH integrand between 5 and 50 MeV to an overall accuracy of about 5% or better, assuming a beam of 1 x 10^7 γ/s with ~5% energy spread.

Besides being a crucial piece of the world's data on the GDH sum rule, the integrand will provide important tests of potential and EFT calculations, being more sensitive to spin physics and relativistic contributions than any previously measured observable.

Anticipated schedule

The HIFROST target will be installed in the fall of this year.

We (the GDH @HIγS Collaboration) expect to begin taking data in early 2010, with preliminary results between 5 and 50 MeV by the end of the year.

<u>Special thanks to</u>: Mohammad Ahmed, Matthew Blackston, Don Crabb, Blaine Norum and Rob Pywell

Two Bunch Mode

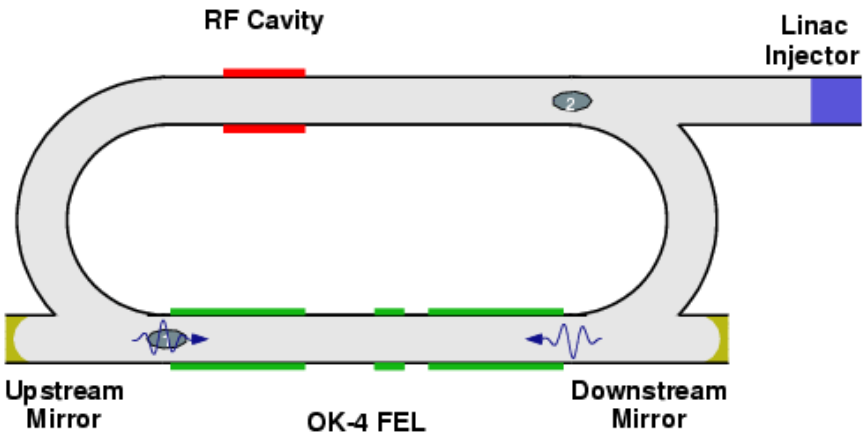

Created by Brent Perdue, 2005

d(γ,n)p @ 14 MeV

red – theory results of Arenhovel;

blue – TME fit to data

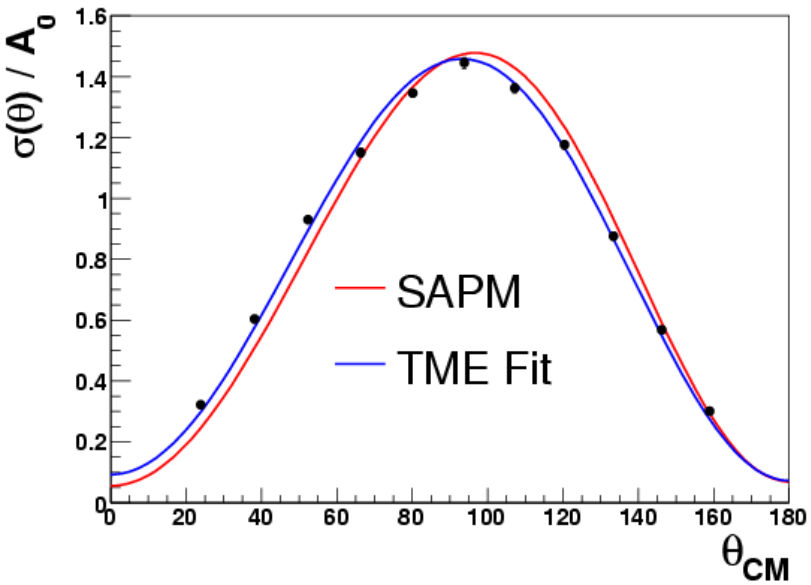

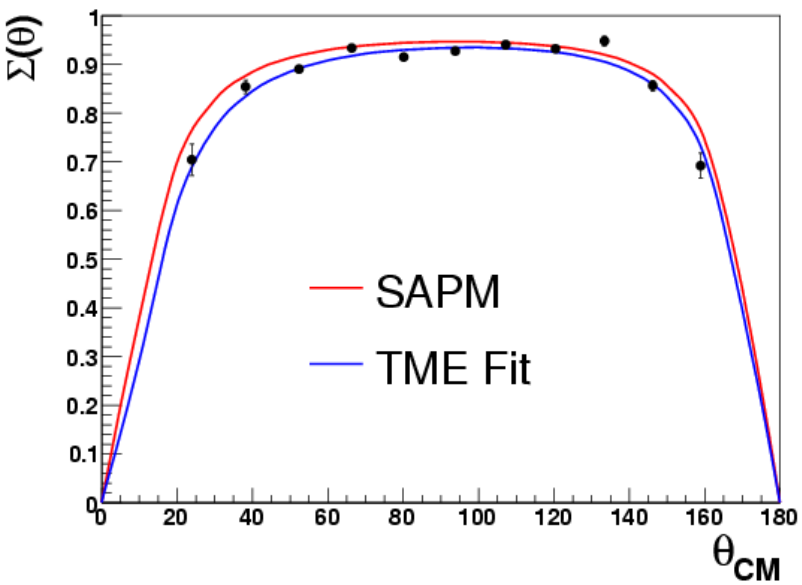

$$\sigma_P - \sigma_A = \frac{3}{4}\,\sigma_T \quad \Big[\, -|{}^1s_0(M1)|^2$$

$$- |{}^3p_0(E1)|^2 \quad - \frac{3}{2}|{}^3p_1(E1)|^2 \quad + \frac{5}{2}|{}^3p_2(E1)|^2$$

$$- \frac{3}{2}|{}^3d_1(E2)|^2 \quad - \frac{5}{6}|{}^3d_2(E2)|^2 \quad + \frac{7}{3}|{}^3d_3(E2)|^2 \,\Big]\,.$$

First determination of the splittings in the p-wave (E1) amplitudes in photodisintegration of the deuteron

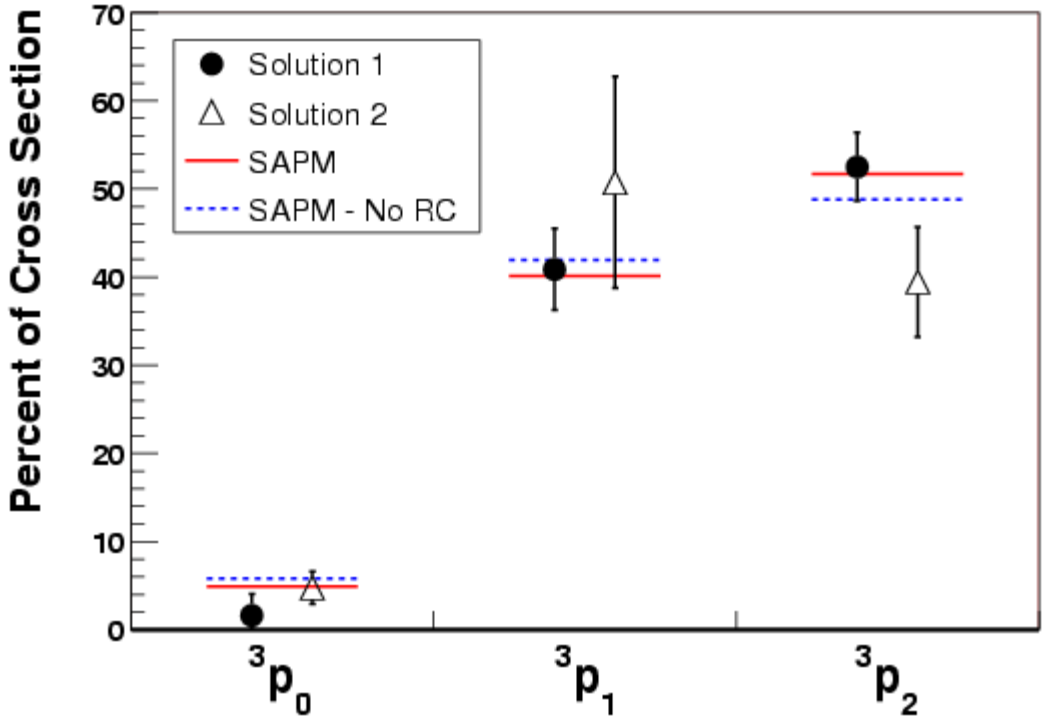

The prediction for the GDH integrand at higher energies

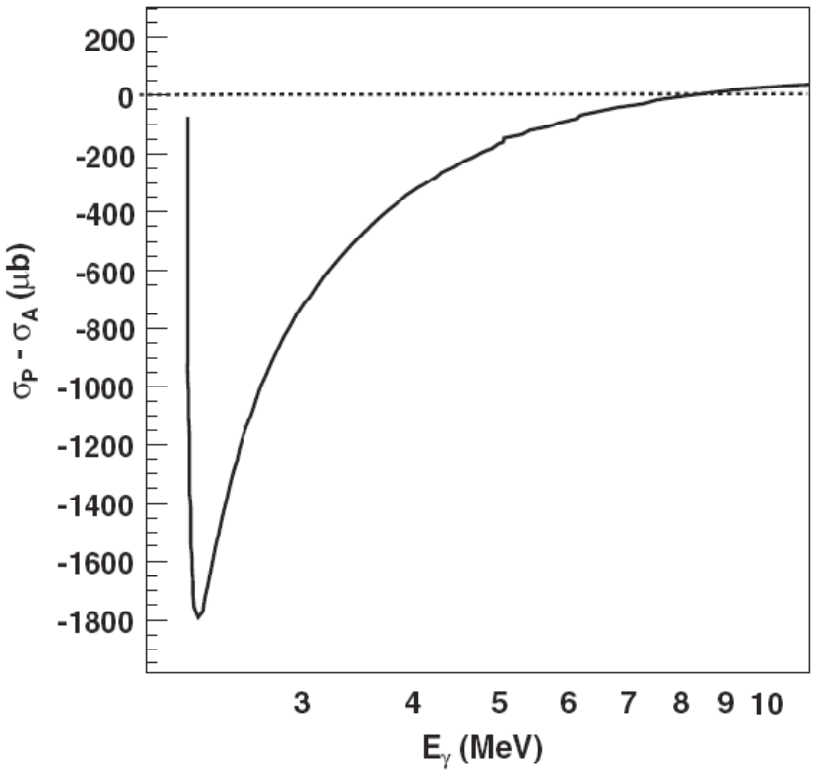

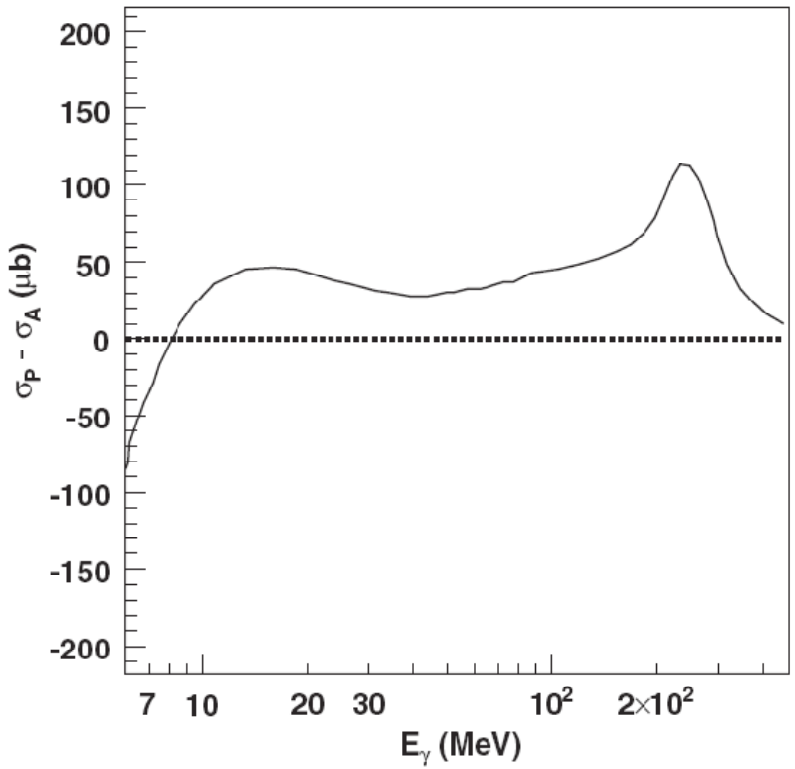

The additional (small) effect of the relativistic contribution, which causes an increase in the $^3p_2$ term relative to the $^3p_0$ and $^3p_1$ terms, is slightly favored by the set of amplitudes labeled Solution 1 (see the $^3p_2$ amplitude at 16 MeV), although just marginally within the error bars.

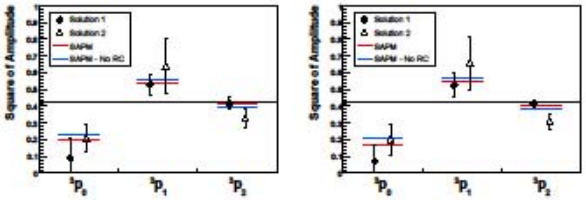

(a)14 MeV (b)16 MeV

FIG. 7: (Color online) Square of the triplet $E1$ p-wave amplitudes as extracted from the data and compared to the SAPM calculation. The solid red line is the prediction from the full SAPM calculation and the dashed blue line is the prediction for the calculation without the inclusion of relativistic contributions (RC). The thin solid line which extends across the entire plot indicates the values that the squares of the amplitudes would have if there no p-wave splitting. Error bars are statistical only.

Figure 8 shows that the $E2$ d-waves take on systematically larger values than expected by the theory for these energies. However, the error bars are so large that most of the points overlap the theoretical values. As already mentioned, the difference in the d-waves is responsible for the difference observed in the fore-aft asymmetry between the theory and the data for the unpolarized cross section (see Figures 5 and 6). Although they are small in magnitude, the d-waves interfere with the dominant p-wave amplitudes to affect the angular distribution.

VII. THE GERASIMOV-DRELL HEARN SUM RULE

Using the formalism of [17], σ_P-σ_A, which enters into the GDH sum rule integrand, can be written in terms of the TME amplitudes extracted from the fits to the data. At these energies, which are near where the integrand is predicted to change from negative to positive,